



## Improving adherence to a daily PrEP regimen is key when considering long-time partnerships

S. J. Gutowska, K. A. Hoffman & K. F. Gurski

**To cite this article:** S. J. Gutowska, K. A. Hoffman & K. F. Gurski (2024) Improving adherence to a daily PrEP regimen is key when considering long-time partnerships, *Journal of Biological Dynamics*, 18:1, 2390843, DOI: [10.1080/17513758.2024.2390843](https://doi.org/10.1080/17513758.2024.2390843)

**To link to this article:** <https://doi.org/10.1080/17513758.2024.2390843>



© 2024 The Author(s). Published by Informa UK Limited, trading as Taylor & Francis Group.



Published online: 20 Aug 2024.



Submit your article to this journal



Article views: 192



View related articles



View Crossmark data

# Improving adherence to a daily PrEP regimen is key when considering long-time partnerships

S. J. Gutowska<sup>a</sup>, K. A. Hoffman<sup>a</sup> and K. F. Gurski<sup>b</sup>

<sup>a</sup>Department of Mathematics and Statistics, University of Maryland Baltimore County, Baltimore, MD, USA;

<sup>b</sup>Department of Mathematics, Howard University, Washington, DC, USA

## ABSTRACT

A population model of HIV that includes susceptible individuals not taking the pre-exposure prophylaxis (PrEP), susceptible individuals taking daily PrEP, and infected individuals is developed for casual partnerships, as well as monogamous and non-monogamous long-term partnerships. Reflecting the reality of prescription availability and usage in the U.S., the PrEP taking susceptible population is a mix of individuals designated by the CDC as high and low risk for acquiring HIV. The rate of infection for non-monogamous long-term partnerships with differential susceptibility is challenging to calculate and requires Markov chain theory to represent the movement between susceptible populations before infection. The parameters associated with PrEP initiation, suspension and adherence impact both the reproduction number of the model and the elasticity indices of the reproduction model. A multi-parameter analysis reveals that increasing adherence has the largest effect on decreasing the number of new infections.

## ARTICLE HISTORY

Received 28 February 2024

Accepted 14 July 2024

## KEYWORDS

HIV; PrEP; Markov chain; reproduction number; elasticity

## 2020 MATHEMATICS

### SUBJECT

### CLASSIFICATIONS

92C60; 92-10; 37N25

## 1. Introduction

The Centers for Disease Control and Prevention (CDC) estimates that over 1.2 million adults and adolescents in the United States (U.S.) are currently living with HIV. The CDC estimates that MSM (gay and bisexual men, transgender women, and others who were born male and who have sex with men but who may or may not identify as gay or bisexual) make up approximately 2% of the total U.S. population and are the population most affected by HIV. In 2019, according to the CDC, 36,801 people received an HIV diagnosis in the U.S. and dependent areas [1] and gay and bisexual men, in particular, accounted for 69% of the overall total [2–4]. Although HIV testing and promotion of condom use will always be core strategies for reducing risk of infection, a more radical approach is needed for HIV-negative people at high risk, whose condom use is inconsistent. One such approach is to encourage the use of pre-exposure prophylaxis (PrEP), a daily oral medication regimen [5] first approved in 2012 by U.S. Food and Drug Administration (FDA). In three observational studies and 15 randomized controlled trials, including iPrEx, PROUD, and IPERGAY of

---

**CONTACT** K. F. Gurski  kgurski@howard.edu  Department of Mathematics, 204 Academic Service Building B, Washington, D.C. 20059, USA

© 2024 The Author(s). Published by Informa UK Limited, trading as Taylor & Francis Group.

This is an Open Access article distributed under the terms of the Creative Commons Attribution License (<http://creativecommons.org/licenses/by/4.0/>), which permits unrestricted use, distribution, and reproduction in any medium, provided the original work is properly cited. The terms on which this article has been published allow the posting of the Accepted Manuscript in a repository by the author(s) or with their consent.

daily oral PrEP have shown that, when taken consistently and correctly, PrEP is extremely effective and reduces the chances of HIV infection to near-zero [6–8]. The effectiveness of PrEP is closely linked to adherence – if a person taking PrEP regularly misses the daily dose, their risk of HIV infection increases significantly. However, daily adherence can be challenging due to side effects [9]. The term adherence is defined by WHO as ‘the extent to which a person’s behaviour – taking medication, following a diet, and/or executing lifestyle changes, corresponds with agreed recommendations from a health care provider [10]’. The WHO document emphasizes the difference between the idea of adherence and compliance and states that ‘the main difference is that adherence requires the patient’s agreement to the recommendations’.

Current guidelines and recommendations for PrEP use include MSM as one of the priority populations for PrEP implementation. In these guidelines, PrEP is indicated for MSM who are at ‘substantial risk’ of infection, defined primarily by four behavioural criteria: unprotected anal intercourse (UAI) in HIV status-unknown monogamous partnerships, UAI outside of monogamous partnership, and anal intercourse in a known-serodiscordant (mixed HIV status) partnership [11], or have had a sexually transmitted infection (STI) with syphilis, gonorrhea, or chlamydia within the past 6 months [12]. Although approximately 25% of HIV-uninfected MSM aged between 18 and 59 years, who report past-year sex, meet indications for PrEP use, current PrEP treatment coverage among MSM is well below the half million who are eligible [13]. Understanding the impact of increased PrEP initiation on population-level HIV incidence should help the public health officials with improving the PrEP awareness, administration, and adherence. Note that the CDC description for the term coverage is ‘the proportion of MSM with indications who start PrEP’ [14] (see Table 1 for a summary of ‘Scenario Definitions for Models of PrEP in MSM Based on CDC Guidelines for Behavioral Indications’). In addition, as of 2024, the CDC has paused PrEP coverage reporting to determine the best methodology for calculating PrEP coverage. Coverage reporting will be resumed in June 2025 with updated PrEP coverage estimates using updated methods and sources [15].

A variety of mathematical models have been used around the world to study HIV transmission dynamics in the presence of PrEP. For instance, Kim et al. [16] in South Korea, Punyacharoen et al. [17, 18] in the UK, and Li et al. [19] in China, used compartmental mathematical models with varying number of compartments based on the stages of disease progression, disease diagnosis and treatment. Silva and Torres [20] focussed on the population of Cape Verde. Chazuka [21] showed that a non-constant population with two susceptible classes, three infected classes, and three treatment classes exhibits a backward bifurcation if the PrEP effectiveness is not 100%. Tollett et al. [22] found a backward bifurcation in a similar model. Recently, Steinegger et al. [23] used network models and data from MSM communities in 58 countries to demonstrate that the efficacy of PrEP is the best strategy for reducing HIV spread, and that targeting those at highest risk is optimal only if the efficacy of PrEP is above a critical value, determined based on various factors, such as effective prevalence. Alternatively, Jenness et al. [14], in the U.S., used a network-based model in which uniquely identifiable sexual partnership dyads were simulated and tracked over time. The findings published by all of the authors confirmed that PrEP reduced the spread of HIV.

Many studies (for example, Hansson et al. [24], Jenness et al. [14], Tollett [25], Tollett et al. [22]) separate the population into *high risk* or *low risk*. While high risk has been

**Table 1.** Parameters pertaining to *PSI* model and partnerships.

Parameter	Description	Value	Ref
$\mu$	Population birth/death rate	1/61 (1/years)	[4]
$\alpha$	New recruited PrEP user fraction	0.01	Proposed
$\theta$	Rate of initiating PrEP	0.05	[3]
$\sigma$	Rate of suspending PrEP	0.2	[44]
$q$	Level of adherence to PrEP treatment	50%	[45]
$r$	PrEP effectiveness	99%	[11, 46]
$\lambda$	Rate of infection	Variable	Derived
$z$	Average number of casual partners per year	6.1/year	[47]
$\bar{z}$	Average number outside partnership casual sexual acts	2/year	[47]
$\beta$	Transmission rate per sexual act	0.002	Calculated
$\tau$	Mean duration of long-term partnership	3.57 (years)	[48]
$\frac{p}{\tau}$	Average number of long-term partners per year	0.210/year	Calculated
$n$	Number of sexual acts over duration of long-term partnership	68 $\tau$	[47]
$c_{eff}$	Condom effectiveness	67.5%	[49]
$u_z$	Condom usage by casual-term partners	80%	[47]
$u_p$	Condom usage by long-term partners	20%	Estimated
$\xi$	Average probability of non-exclusivity	0.264	[48]
$I_0$	Initial percentage infected (2005)	9%	Calculated
$P_0$	Initial percentage on PrEP (2012)	0.2 %	Calculated

defined by the CDC [11], the idea of risk varies by individual. In their work, Whitfield et al. [26] pointed out that the risk perception (i.e. whether the person views themselves as an appropriate candidate) has been identified as a barrier to increased PrEP initiation. If individuals do not see themselves as someone for whom PrEP is intended, they are less likely to start a regimen. Furthermore, a change in risk perception could lead to discontinuation of the treatment all together, regardless of actual changes in risk behaviour. This suggests that the idea of distinguishing between the high and low risk behaviour might not be enough when considering the best strategies to combat poor adherence. In addition, a study by Weiss et al. [27] with 3508 sexually active, HIV-negative MSM, 34% met these indications for PrEP use. Nearly 40% of those currently using PrEP did not meet indications for PrEP, and 68% of MSM with indications for PrEP were not currently using PrEP. This indicates that PrEP users are not all high risk and not all high risk individuals are taking advantage of PrEP.

Rosenberg et al. [28] analysed data from the first MSM cycle of the CDC National HIV Behavioral Surveillance system, conducted from 2003 to 2005, and concluded that among 11,191 sexually active MSM, 32% reported having only male casual partners, 44% had main (long-term) and casual partners, and 24% were in a monogamous partnership. Updated results were published by Chapin-Bardales et al. [29], who used CDC's National HIV Behavioral Surveillance data from 2008, 2011, and 2014, to study trends in the number and partner type composition (long-term/casual) of male sex partners among 28,061 U.S. MSM. This indicates that a model for PrEP in the U.S. MSM community needs to

capture long-term partnerships. Population models for sexually transmitted infections have traditionally fallen into two categories: casual partnerships with an inherent partnership length of zero or pair formation models that capture the duration of the partnerships. The casual partnership model approximates the transmission rate as the product of the transmission probability per sexual act, the probability of a random sexual partner being infected, and the rate of sexual acts. In contrast, pair formation models (see, for example, the review by Kretzschmar and Heijne [30]), track disease transmission through pairs with possible transmission occurring in an established partnership with one infected and one susceptible individual. These models track pair formation and dissolution, as well as disease transmission. Pair formation models can capture non-monogamous transmission, but at the expense of needing a moment closure method [31] to capture the interaction sexual exchanges outside the monogamous relationship. These pair-formation models do not scale well as each model must contain sub-populations of each single or pair combination. Gurski [32] developed a non-pair formation population model that accounts for the possibilities of an infection from either a casual sexual partner or a long-term partner who was either infected at the start of the partnership or newly infected. The model allows for multiple long-term partnerships, which include serially monogamous and concurrent partnerships without needing to explicitly track pairs. Instead, the impact of the long-term partnerships on the rate of infection is captured by calculating the expected values of these extended contacts. The results in Gurski et al. [33] show that the long-term partnership model and the pair formation model give similar results, but the long-term partnership model has fewer equations.

As evidenced above, researchers around the world have been estimating the potential impact of PrEP under different intervention scenarios, examining the relative importance of implementation strategies and individual adherence. One of the earliest PrEP models, presented by Gomez et al. [34] in 2012, shows an important epidemiological impact of PrEP use, largely driven by the characteristics of the implementation programme, such as PrEP conditional efficacy, coverage, prioritization strategy, and time to scale up, as well as risk compensation behaviour. Hansson et al. [24] included different types of partnerships in a pair-formation model including a level of sexual activity, but the assumption of individuals never stopping or deviating from the strict PrEP regimen is unrealistic considering the data [2].

In our work, we address multiple susceptible populations with an additional distinction between the ‘types’ of partnerships among the MSM population. We develop an analytic model of the spread of HIV with the implementation of PrEP in a homogeneous (sexually-active MSM) population with the novel feature of different partnership scenarios, including casual and non-monogamous long-term partnerships. Among the many parameters, the presented model takes into account rates of acquiring new partners, duration of the long-term partnerships, rates at which susceptible individuals initiate and suspend the pre-exposure prophylaxis programme, treatment adherence rate and effectiveness rate of PrEP. We begin with a calculation of the probability that an uninfected partner, who is acquired at time  $\kappa$ , remains uninfected and then combine it with the probability of staying in that partnership until the later time of infection  $t$ . Our goal is to calculate the probabilities of staying clear of infection during the time between  $\kappa$  and  $t$ , and, at the same time, to account for the possibility of a susceptible long-term partner either starting or stopping PrEP treatment. Capturing the impact of newly infected non-monogamous long-term

partners on the spread of HIV is a non-trivial task since there are two susceptible populations, those who are not taking PrEP and those who are taking PrEP (even perfect adherence cannot remove all risk). To accomplish our goal, we will turn to the Markov chain theory. More specifically, we take a novel approach to apply the susceptible-illness-death theory of Markov chains with time-constant hazards to our situation with two classes with differential susceptibility and one illness class. Stochastic processes have been used to model disease dynamics. In the last few decades, researchers around the world have used state-based models and discrete Markov chains to study progression of HIV, both without [35–37] and with PrEP [38]. We utilize the continuous-time Markov chain only to help us derive the rate of infection arising from the non-monogamous long-term partnerships. Our previous work confirms that considering only casual partnerships does not provide an accurate representation of the disease progression over long time periods [39]. Hence the inclusion of non-monogamous long-term partnerships is needed to accurately model the spread of HIV.

Adherence plays a very important role, possibly even more important than just increasing the number of individuals starting PrEP. Simpson and Gumel [40] presented a model with casual partnerships, stratifying the susceptible population using PrEP based on two levels (low and high) of treatment adherence. In contrast, our adherence parameter  $q$  varies continuously between 0 and 1. This adjustment should reflect behavioural and societal factors influencing adherence rates vary with geography and culture. Even within the same geographic region, different subpopulations may exhibit different rates of adherence to PrEP, which may make it difficult to develop a generalized model of adherence [41]. In addition, we are able to determine the level of adherence necessary to lower the reproduction number to  $\mathcal{R} < 1$  for ranges of PrEP initiation and discontinuation rates. The basic reproduction number is the average number of secondary infections produced by a typical case of an infection in a population where everyone is susceptible. This situation is no longer applicable to the availability of PrEP because the individuals on PrEP do not have the same level of susceptibility. Hence, our notational choice  $\mathcal{R}$  rather than  $\mathcal{R}_0$ , reflects that the model is better described by an effective reproduction number as some individuals may no longer be susceptible [42]. In this work, we illustrate that PrEP initiation has a larger effect on the reproduction number than does discontinuation, although discontinuation is important.

The model and results of this paper will be presented as follows. In Section 2, we describe the *PSI* (PrEP-treated, susceptible, infected) model and in Section 3 consider three cases based on the type of partnership(s) and then calculate the corresponding rates of infection and reproduction numbers. In Section 4, we describe the choice of parameter values for the MSM community in the U.S. from 2005 to 2025. We provide a comparison between CDC measurements of prevalence, incidence, and percentage of MSM on PrEP with our model predictions in Section 5. Sections 6 and 7 contain the effect of the rate of PrEP initiation, the rate of PrEP discontinuation, and the adherence level on the reproduction number and its elasticity. We conclude in Section 8 with a discussion.

## 2. The model

We extend the standard SI model by adding a new group of susceptibles,  $\tilde{P}$ , namely the individuals who are using PrEP. The population being modelled here consists of sexually

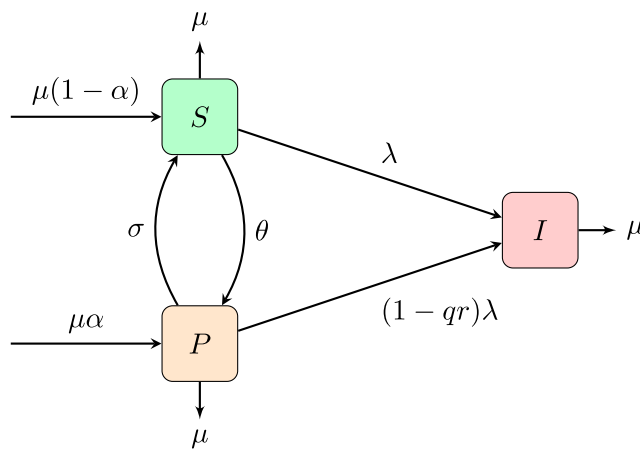


**Figure 1.** Schematic diagram of the  $PSI$  model with three groups, the fraction of infected individuals in  $I$ , the fraction of susceptible individuals in  $S$  who are not currently using PrEP and may become infected at a rate  $\lambda$ , and the PrEP users in group  $P$  who may become infected at a modulated rate  $(1 - qr)\lambda$ . The reduction in infectivity of  $P$  is due to effectiveness of PrEP treatment  $r$ , and an adherence to the treatment  $q$ . The parameters  $\theta, \sigma$ , and  $\mu$  correspond to the PrEP initiation rate, PrEP suspension rate, and population removal rate (for constant population also the population addition rate), respectively.

active MSM individuals, regardless of their HIV status or qualifications for PrEP. We divide the total constant population,  $N_0$ , into two susceptible groups and one infected group. The susceptible individual cannot spread the disease and is either currently taking PrEP (group  $\tilde{P}$ ) or is not taking PrEP but might be a possible candidate for it (group  $\tilde{S}$ ). The infected individual (group  $\tilde{I}$ ) contracted HIV, and can spread the disease. There is only one infectious group because we do not distinguish between acute and chronic/latent phases of infection. For the simplicity of work that follows, it is convenient to transform the system  $\tilde{P}\tilde{S}\tilde{I}$  into an equivalent model with proportions  $P = \tilde{P}/N_0$ ,  $S = \tilde{S}/N_0$ , and  $I = \tilde{I}/N_0$  denoting fractions of the classes  $\tilde{P}$ ,  $\tilde{S}$ , and  $\tilde{I}$  in the constant population  $N_0$ , and satisfying  $P + S + I = 1$ .

To maintain a system that is easier to analyse, we currently do not account for differences based on race, age or other demographic factors within the population. Individuals join the sexually active population at a rate  $\mu$ . To explore the possible effect of introducing PrEP to the susceptible population before they become sexually active, we introduce a parameter  $\alpha$ . Assuming  $\alpha$  is a proportion of those starting PrEP before they become sexually active, the individuals enter the model (Figure 1) either through the group  $P$ , at a rate  $\mu\alpha$ , or the group  $S$ , at a rate  $\mu(1 - \alpha)$ . People move from  $S$  to  $I$  at a rate of infection  $\lambda$ . However, the rate of infection at which people move from  $P$  to  $I$  is modulated by a factor  $(1 - qr)$ , which represents the degree of protection of PrEP users. Following the CDC descriptions for the term adherence (See [14], Table 1 for a summary of these Scenario Definitions for Models of PrEP in MSM Based on CDC Guidelines for Behavioral Indications), we define  $q$  to be the average adherence to the daily PrEP regimen and  $r$  to be the treatment effectiveness of PrEP in preventing HIV if taken with 100% adherence ( $q = 1$ ).

In addition, the susceptible individual in  $S$  who qualifies for and starts PrEP treatment moves to  $P$  at a rate of  $\theta$ . At the same time, the people in  $P$  who stop the treatment move back to  $S$  at the rate of  $\sigma$ . Each group can be exited due to natural death, migration, or

changes in sexual behaviour, at a combined inflow/outflow rate  $\mu$ . The inflow and outflow rates are equal for a constant population. We assume that the individuals diagnosed as HIV positive have ready access to highly effective HAART treatment. HAART treatment cannot cure HIV; it can, however, delay or prevent the onset of symptoms or progression to AIDS, thereby prolonging survival in people infected with HIV [43]. With that in mind, we do not consider death or other removal from population due to disease. The equations governing the model in Figure 1 are given by

$$\begin{aligned}\frac{dP}{dt} &= \mu\alpha + \theta S - (1 - qr)\lambda P - (\sigma + \mu)P, \\ \frac{dS}{dt} &= \mu(1 - \alpha) + \sigma P - \lambda S - (\theta + \mu)S, \\ \frac{dI}{dt} &= \lambda S + (1 - qr)\lambda P - \mu I.\end{aligned}\quad (1)$$

The parameters present in the Figure 1 and in the model Equation (1) are listed in Table 1. The chosen values for the rates of initiating ( $\theta$ ), suspending ( $\sigma$ ), and adherence ( $q$ ) to the PrEP treatment, are addressed in Section 4, where we discuss all parameters in the light of current literature.

### 3. Partnership models and the rate of infection $\lambda$

In this section, we consider two different types of partnerships: casual partnerships and long-term partnerships, as well as combinations of those partnership models. Casual partnerships are the basis for classical epidemiological models that rely on the law of mass action. For sexually transmitted diseases, the effect of long-term partnerships and combinations of long-term partnerships with casual encounters become important to represent disease dynamics [32, 33, 39, 50]. In this section, we compute the rate of infection  $\lambda = \lambda_z + \lambda_p^I + \lambda_p^{S/P}$ , where  $\lambda_z$  represents the infection rate from casual-only relationships,  $\lambda_p^I$  represents the infection rate from long-term monogamous partnerships, and  $\lambda_p^{S/P}$  represents the rate of infection from potentially non-monogamous long-term partnerships. The calculation of the rate of infection is complicated by having two different susceptible states, which an individual may transition between before becoming infected, and having long-term partnerships in the model. The rate of infection for models that include long-term partnerships is defined to be an expected value. We use Markov chain theory to define the expected value to be the integral of the product of the probability of being in one of the susceptible states and the instantaneous transition rate, integrated with respect to a probability distribution. Hence, the calculation of the rate of infection from long-term non-monogamous partnerships becomes more complicated than the previous two cases because both partners can transition between the two susceptible states  $S$  and  $P$  and we are including long-term partnerships.

#### 3.1. Casual-only partnerships: $\lambda_z$

We consider a susceptible individual of interest,  $X$ , who is not in any long-term partnership but engages only in casual sexual behaviour. The infection rate from casual partners,

denoted  $\lambda_z$ , follows the classic law of mass action with a zero inherent length infection contact. It assumes that the transmission rate from an infected individual in  $I$  is  $z\beta c_z$ , where  $z$  is the rate of casual sexual encounters and  $\beta$  is the transmission probability per sexual encounter with an infected individual. The transmission reduction factor term due to condom use,  $c_z$  is defined as  $c_z = 1 - c_{eff} \cdot u_z$ , where  $c_{eff}$  is a condom effectiveness and  $u_z$  is the probability of a condom being used in a casual partnership. The infection rate from casual partners,  $\lambda_z$  is calculated as

$$\lambda_z = z\beta c_z I, \quad (2)$$

where  $I$  denotes the ‘infected’ (HIV-positive) fraction of the population.

### 3.2. Long-term partnerships with infected individual: $\lambda_p^I$

Next, we consider a susceptible individual of interest,  $X$ , who is in a monogamous long-term partnership with infected individual  $Y$ . The individual  $X$  does not engage in any casual sexual behaviour outside of this partnership. Since there are no casual sexual acts, the susceptible individual can only become infected through his infected long-term partner. We define the rate of infection  $\lambda_p^I$  as the expected value  $\chi E[I]$ . Here,  $\chi$  represents the transmission rate of infection within a long-term partnership. This derivation appeared in [39], but is reproduced here for readability. We include a transmission reduction factor term due to condom use,  $c_p = 1 - c_{eff} \cdot u_p$ , where  $u_p$  is the probability of a condom being used in a long-term partnership. The probability of not being infected in a single act is then  $(1 - c_p\beta)$ , and the probability of not being infected after  $n$  sexual acts with the infected long-term partner are  $(1 - c_p\beta)^n$ . The exponent  $n$  reflects the number of exposures over the duration of the long-term partnership with the infected partner. In  $\lambda_z$ , we used the average *rate* of casual encounters per year,  $z$ . However, in  $\lambda_p$  we use the rate of acquiring long-term partners  $p/\tau$  (per partnership duration), where  $p$  represents the average of the total *number* of long-term partners and  $\tau = 1/(b + 2\mu)$  represents the average long-term partnership duration, with  $\mu$  being the removal rate from the sexually active population and  $b$  denoting the rate at which long-term partnerships dissolve. Then the probability that the susceptible long-term partner will be infected after  $n$  sexual acts with the long-term partner in  $I$  is our rate of transmission  $\chi = (p/\tau)(1 - (1 - c_p\beta)^n)$ . The parameters included in the derivation of the rate of infection for this case are listed in Table 1.

When deriving the rate of infection  $\lambda_p^I$  from an infected partner, we assume that the infected partner has not transmitted the infection before a given time  $t$ . In short, the rate of infection by the fraction of infected long-term partners out of the total population is the expected value of the rate of infection due to partners initially chosen while infectious,  $\lambda_p^I = \chi E[I]$ . In this case, the expected value is

$$E[I] = \int_{-\infty}^t \frac{I(\kappa)}{\tau} e^{-(t-\kappa)/\tau} d\kappa, \quad (3)$$

where we have accounted for the probabilities given as **Prob 1** and **Prob 2**:

**Prob 1** The probability that a partner acquired at time  $\kappa$  was already infected:  $P(X(\kappa) \in I) = I(\kappa)$ .

**Prob 2** The probability that a partner acquired at time  $\kappa$  will still be a partner at time  $t$ :  $P(X(t) \in \text{Partner})$ . We assume that the probability of the partnership lasting through time  $t$  can be described by a distribution function that is a decaying exponential scaled by the length of an average long-term partnership,  $\tau$ ,

$$P(X(t) \in \text{Partner}) = \frac{1}{\tau} e^{-(t-\kappa)/\tau}.$$

To simplify this nonlinear and non-local problem, we replace  $I(\kappa)$  with its linear approximation:  $I(\kappa) \approx I(t) + I'(t)(\kappa - t)$ , and use the derivative  $I'(t) = \lambda S(t) + (1 - qr)\lambda P(t) - \mu I(t)$  directly from our ODE model Equation (1). The approximation is  $I(\kappa) \approx (1 + \mu\tau)I(t) - \lambda\tau S(t) - \lambda\tau(1 - qr)P(t)$  in the integrand of (3). In other words, we are approximating the fraction of infectious individuals  $I(\kappa)$  at time  $\kappa$  as the fraction of infected at time  $t$  plus the fraction of infected who died,  $(1 + \mu\tau)I(t)$ , and subtracting off the fraction of the individuals,  $\lambda\tau(S(t) + (1 - qr)P(t))$ , who became infected between times  $\kappa$  and  $t$ , with  $\tau = t - \kappa$  denoting the period between the start of long-term partnership and the time of infection. Therefore, we can write (3) as

$$\begin{aligned} E[I] &= \int_{-\infty}^t \frac{I(\kappa)}{\tau} e^{-(t-\kappa)/\tau} d\kappa \\ &\approx \frac{1}{\tau} [(1 + \mu\tau)I(t) - \lambda\tau S(t) - \lambda\tau(1 - qr)P(t)] \int_{-\infty}^t e^{-(t-\kappa)/\tau} d\kappa \\ &= (1 + \mu\tau)I(t) - \lambda\tau[S(t) + (1 - qr)P(t)], \end{aligned}$$

and the rate of infection from the infected long-term partner is

$$\lambda_p^I \approx \chi \left( (1 + \mu\tau)I(t) - \lambda\tau[S(t) + (1 - qr)P(t)] \right). \quad (4)$$

### 3.3. Potentially non-monogamous long-term partnerships: $\lambda_p^{S/P}$

Finally, we include both casual and long-term partnerships in the same model. We consider a susceptible individual of interest,  $X$ , who is in a long-term partnership with individual  $Y$  but at the same time both  $X$  and  $Y$  may have sexual encounters with other infected individuals, outside of their long-term partnership. The long-term partnership we are considering was formed when both  $X$  and  $Y$  are susceptible. In this instance,  $Y$  may get infected through an outside-the-partnership sexual encounter and then, subsequently,  $Y$  may infect his susceptible long-term partner  $X$ . In this section we compute the rate of infection due to the initially susceptible long-term partner  $Y$ , denoted by  $\lambda_p^{S/P}$ . The parameters used in this case are included in Table 1. We define  $\lambda_p^{S/P}$  as a product of the transmission rate  $\psi$  and the fraction of the newly infected (i.e. susceptible at the time of partnership formation,  $\kappa$ ) individuals  $I^{new}$  at time  $t$ . To account for the changes in the number of infected individuals during the time between the start of the long-term partnership  $\kappa$  and the time of infection  $t$ , we will use the mean (expected value) of the fraction of newly infected individuals,

represented as a function of a continuous random variable  $T$ ,

$$\lambda_p^{S/P} \equiv \psi E[I^{new}(T)]. \quad (5)$$

We consider four possible scenarios to account for the fact that we have two uninfected groups, namely susceptibles  $S$ , who are not in treatment, and susceptible PrEP users  $P$ . The individual  $Y$  may start in one of these groups but possibly transition to the other one before actually becoming infected. We will determine the following four rates of infection:  $\lambda_p^{SS}$ , which represents the infection rate for an individual  $Y$  is in  $S$  at the start of the long-term relationship as well as at time of infection;  $\lambda_p^{SP}$ , which represents the infection rate for an individual  $Y$  who is in state  $P$  at the start of the long-term relationship but suspends PrEP treatment and transitions to  $S$  and remains there at the time of infection;  $\lambda_p^{PP}$  represents the rate of infection for an individual  $Y$  who is taking PrEP at the start of the long-term relationship and at the time of infection; and  $\lambda_p^{PS}$ , which represents the rate of infection of an individual  $Y$  who is in  $S$  at the start of the relationship but initiates PrEP treatment and remains on the treatment at the time of infection. The total rate of infection from the initially susceptible partner is the combination  $\lambda_p^{S/P} = \lambda_p^{SS} + \lambda_p^{SP} + \lambda_p^{PP} + \lambda_p^{PS}$ .

The calculation of the expected value of the fraction of newly infected individuals in each of the scenarios will consist of calculating the following probabilities **Prob 3–Prob 5**.

**Prob 3** *Probability that  $Y$  was susceptible at time  $\kappa$ .*

**Prob 4** *Probability that an uninfected long-term partner  $Y$  ‘survives’ as such through time period between  $\kappa$  and  $t$ .* This probability is a product of two probabilities (survival functions), since staying in the partnership and avoiding infection are two independent events:

- (a) (a) *Probability that  $Y$  is in state  $k$  at time  $t$ , given  $Y$  was in state  $j$  at time  $\kappa$ :*  $P_{jk}(t - \kappa) = P\{Y(t) = k | Y(\kappa) = j\}$ , where  $j, k \in P, S$ . This probability, of not getting infected during the  $(\kappa, t)$  time period, is represented by a survival function and will be calculated later in this section as a transition probability in a multi-state model.
- (b) (b) *Probability that  $Y$  is still a partner at time  $t$ .* This is the same as **Prob 2** in the calculation of the rate of infection for the monogamous long-term partnerships.

**Prob 5** *Probability that initially susceptible partner  $Y$  becomes infected at time  $t$ , while being in group  $j \in P, S$ .* This probability is a transition rate (time-constant hazard) from  $j$  to  $i$ , denoted by  $\rho_{ji}$ , with  $j \in P, S$ . See Figure 2 for an illustration of these time-constant transition-specific hazard rates.

The remainder of this section provides the background and calculation of **Prob 4a** and **Prob 5**.

### 3.3.1. Markov chain theory

A standard statistical model specifies the state structure and the form of the hazard function for each possible transition. The transition-specific hazard functions are the instantaneous rates of transitioning among the susceptible PrEP-taking population, susceptible population not taking PrEP, and the infected population (see Figure 2). To look several steps

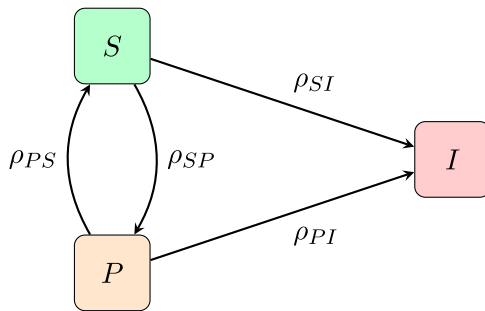


**Figure 2.** Schematic diagram of the three-state Markov chain model with time-constant transition-specific hazard rates  $\rho_{jk}$  for  $j, k \in P, S, I$ . The transition-specific hazard functions reflect the trigger ('hazard') of the next transition.

(state transitions) ahead, we must consider the transition probability, that is, the probability of being in a given state at a given time, possibly conditioned on what has happened until some time point. Therefore, the transition probabilities are the keys to making long-term predictions. A complete multi-state model analysis includes an investigation of the hazard rates and the transition probabilities. In this work, we discuss these quantities in a time-constant hazard setting, which makes the derivation of closed mathematical forms for the transition probabilities feasible [51]. We utilize the continuous-time Markov chain to derive the rate of infection. The idea behind Markov chains can be summarized as follows: 'conditioned on the current state, the past and the future states are independent' [52]. Thus, the time that the process spends in each state must have a 'memory-less' property, called the Markov property. In short, the Markov assumption implies that the past state  $Y(\kappa)$  and the future  $Y(t)$  are conditionally independent given the present.

### 3.3.2. Prob 4a: calculation of transition probabilities $\mathcal{P}_{jk}(t - \kappa)$

First, we compute the probability that  $Y$  is in state  $k$  at time  $t$ , given  $Y$  was in state  $j$  at time  $\kappa$ ,  $\mathcal{P}_{jk}(t - \kappa) = \mathcal{P}\{Y(t) = k | Y(\kappa) = j\}$ , where  $j, k \in P, S$  using the theory of Markov chains. Given two time points  $\kappa$  and  $t$ , with  $\kappa < t$ , we write the transition probabilities as

$$\mathcal{P}_{jk}(t - \kappa) = \mathcal{P}\{Y(t) = k | Y(\kappa) = j\}, \quad (6)$$

with  $j, k$  indicating possible states  $\{P, S, I\}$ , as well as the transition matrix,  $\mathbf{P}(t - \kappa)$ ,

$$\mathbf{P}(t - \kappa) = \begin{bmatrix} \mathcal{P}_{PP}(t - \kappa) & \mathcal{P}_{PS}(t - \kappa) & \mathcal{P}_{PI}(t - \kappa) \\ \mathcal{P}_{SP}(t - \kappa) & \mathcal{P}_{SS}(t - \kappa) & \mathcal{P}_{SI}(t - \kappa) \\ \mathcal{P}_{IP}(t - \kappa) & \mathcal{P}_{IS}(t - \kappa) & \mathcal{P}_{II}(t - \kappa) \end{bmatrix}, \quad (7)$$

with each  $\mathcal{P}_{jk}(t - \kappa)$  defined in (6) and illustrated in Figure 2. The transition matrix satisfies  $\mathbf{P}(0) = \mathbf{I}$  and  $\sum_{k \in C} \mathcal{P}_{jk}(t - \kappa) = 1$ , for all  $t \geq \kappa$ . Since the rows of  $\mathbf{P}$  must sum to 1, and there is no transition out of the absorbing state  $I$ , we can write the identities  $\mathcal{P}_{IP} = 0$ ,  $\mathcal{P}_{IS} = 0$ ,  $\mathcal{P}_{II} = 1$ ,  $\mathcal{P}_{PP} + \mathcal{P}_{PS} + \mathcal{P}_{PI} = 1$ , and  $\mathcal{P}_{SS} + \mathcal{P}_{SP} + \mathcal{P}_{SI} = 1$ . Therefore, out of the six non-zero transition probabilities left to determine, only four of them are needed, since the remaining two can be obtained using the four identities listed above.

The transition probabilities  $\mathcal{P}_{jk}(t - \kappa)$  can be calculated from the transition-specific hazard rates [52], so-called intensities  $\rho_{jk}$ , from state  $j$  to state  $k$  by solving the forward

Kolmogorov differential equations [53]

$$P'(t - \kappa) = P(t - \kappa)\mathbf{G}, \quad (8)$$

that state that the rate of change of the probability of transition is equal to the product of the probability of transition and the time-constant hazard rate. The matrix  $\mathbf{G}$  is called the (infinitesimal) generator of the Markov chain and its entries,  $G_{jk}$ , are the time-constant hazard rates  $\rho_{jk}$  with  $j, k \in \mathcal{C}$  [54]. Here  $\mathbf{G}$  is defined to be

$$\mathbf{G} = \begin{bmatrix} \rho_{PP} & \rho_{PS} & \rho_{PI} \\ \rho_{SP} & \rho_{SS} & \rho_{SI} \\ \rho_{IP} & \rho_{IS} & \rho_{II} \end{bmatrix}. \quad (9)$$

Since there is no cure for HIV, there is no ‘return’ from an infected state to any susceptible state, therefore we have  $\rho_{IP} = \rho_{IS} = 0$ . The only non-zero off-diagonal entries are  $\rho_{PS} = \sigma$ ,  $\rho_{SP} = \theta$ ,  $\rho_{PI} = \bar{\lambda}\xi(1 - qr)$ , and  $\rho_{SI} = \bar{\lambda}\xi$ . The first two quantities correspond to the transitions between the two susceptible groups, namely the rates of starting and stopping the PrEP treatment, as described in our system (1) and illustrated in Figure 1. The latter two,  $\rho_{PI}$  and  $\rho_{SI}$ , are the hazard rates corresponding to the transitions into infected state  $I$ , and represent the probabilities that the initially susceptible partner  $Y$  becomes infected, and will also be used in the calculation of a total rate of infection. In both  $\rho_{PI}$  and  $\rho_{SI}$ , it is important to point out the presence of the non-exclusivity parameter,  $\xi$ , as well as a different rate of infection, denoted here by  $\bar{\lambda}$ . This is due to the fact that an initially susceptible long-term partner  $Y$  can only get infected by engaging in sexual activity outside of the long-term partnership, and the chance of that activity taking place is precisely  $\xi$ . The rate of infection from such activity depends on its frequency, and hence includes parameter  $\bar{z}$ , denoting the average annual number of casual partners of  $Y$ , outside of the long-term partnership. We emphasize that  $\bar{z}$  is not necessarily the same as  $z$ , which refers to the average number of casual partners of  $X$ , per year. In addition, since the row sums of  $\mathbf{G}$  are all zero, the diagonal entries, as defined before, are  $G_{jj} = \rho_{jj} = -\sum_{k \neq j} \rho_{jk}$  for  $j, k \in P, S, I$ . Hence, the generating matrix is

$$\mathbf{G} = \begin{bmatrix} -(\sigma + \bar{\lambda}\xi(1 - qr)) & \sigma & \bar{\lambda}\xi(1 - qr) \\ \theta & -(\theta + \bar{\lambda}\xi) & \bar{\lambda}\xi \\ 0 & 0 & 0 \end{bmatrix}. \quad (10)$$

As pointed out before, the transition probabilities,  $\mathcal{P}_{PI}$  and  $\mathcal{P}_{SI}$ , into absorbing state  $I$  can be calculated from the four transition probabilities between the non-absorbing states. Since the exponential terms in Equation (12) correspond to non-zero eigenvalues of the generating matrix  $\mathbf{G}$ , we simplify the model by deleting the absorbing state  $I$ , and hence eliminating the zero eigenvalue. This results in a defective model, where the rows of the reduced generating matrix  $\tilde{\mathbf{G}}$  do not sum to 0, and

$$\tilde{\mathbf{G}} = \begin{bmatrix} -(\sigma + \bar{\lambda}\xi(1 - qr)) & \sigma \\ \theta & -(\theta + \bar{\lambda}\xi) \end{bmatrix}. \quad (11)$$

Since the eigenvalues of  $\mathbf{G}$  are distinct, the solutions for the transition probabilities are

$$\mathcal{P}_{ij}(t - \kappa) = \sum_r a_{jkr} e^{-\omega_r(t-\kappa)}, \quad (12)$$

where the rate constants,  $-\omega_r$ , are the eigenvalues of  $\mathbf{G}$ . This approach reduces the equation in (12) from three to two dimensions, but, since the eigenvalues of  $\tilde{\mathbf{G}}$  are the same as the non-zero eigenvalues of  $\mathbf{G}$ , it still allows us to find  $\mathcal{P}_{PP}$ ,  $\mathcal{P}_{PS}$ ,  $\mathcal{P}_{SP}$ , and  $\mathcal{P}_{SS}$  for our model. The solutions to the differential Equation (8) using (12) are

$$\mathcal{P}_{jk}(t - \kappa) = \alpha_{jk1} e^{-\omega_1(t-\kappa)} + \alpha_{jk2} e^{-\omega_2(t-\kappa)}, \quad (13)$$

with constants  $\alpha_{jk1}$  and  $\alpha_{jk2}$  to be determined. The positive values

$$-\omega_{1,2} = -\frac{1}{2} \left( 2\bar{\lambda}\xi + (\theta + \sigma - \bar{\lambda}\xi qr) \mp \sqrt{(\theta - \sigma + \bar{\lambda}\xi qr)^2 + 4\theta\sigma} \right), \quad (14)$$

are the eigenvalues of the  $2 \times 2$  matrix  $\tilde{\mathbf{G}}$  as well as the non-zero eigenvalues of the  $3 \times 3$  matrix  $\mathbf{G}$ . Using the properties of the probability matrix,  $P(0) = I$  and  $\sum_{k \in \mathcal{C}} \mathcal{P}_{jk}(t - \kappa) = 1$ , for all  $t \geq \kappa$ , we form the system of six linear equations with four unknowns

$$\begin{aligned} -\alpha_{PP1} \omega_1 &= \alpha_{PP1} \rho_{PP} + \alpha_{PS1} \rho_{SP}, & -\alpha_{PS1} \omega_1 &= \alpha_{PP1} \rho_{PS} + \alpha_{PS1} \rho_{SS}, \\ -\alpha_{PP2} \omega_2 &= \alpha_{PP2} \rho_{PP} + \alpha_{PS2} \rho_{SP}, & -\alpha_{PS2} \omega_2 &= \alpha_{PP2} \rho_{PS} + \alpha_{PS2} \rho_{SS}, \\ \alpha_{PP1} + \alpha_{PP2} &= 1, \\ \alpha_{PS1} + \alpha_{PS2} &= 0. \end{aligned} \quad (15)$$

The solution to this linear system determines the values of  $\alpha_{Pjr}$ :

$$\begin{aligned} \alpha_{PS1} &= -\frac{(\rho_{PP} + \omega_1)(\rho_{PP} + \omega_2)}{\rho_{SP}(\omega_2 - \omega_1)}, & \alpha_{PP1} &= \frac{\rho_{PP} + \omega_2}{\omega_2 - \omega_1}, \\ \alpha_{PS2} &= \frac{(\rho_{PP} + \omega_1)(\rho_{PP} + \omega_2)}{\rho_{SP}(\omega_2 - \omega_1)}, & \alpha_{PP2} &= -\frac{\rho_{PP} + \omega_1}{\omega_2 - \omega_1}. \end{aligned} \quad (16)$$

Similarly, from the following six equations,

$$\begin{aligned} -\alpha_{SS1} \omega_1 &= \alpha_{SS1} \rho_{SS} + \alpha_{SP1} \rho_{PS}, & -\alpha_{SP1} \omega_1 &= \alpha_{SS1} \rho_{SP} + \alpha_{SP1} \rho_{PP}, \\ -\alpha_{SS2} \omega_2 &= \alpha_{SS2} \rho_{SS} + \alpha_{SP2} \rho_{PS}, & -\alpha_{SP2} \omega_2 &= \alpha_{SS2} \rho_{SP} + \alpha_{SP2} \rho_{PP}, \\ \alpha_{SS1} + \alpha_{SS2} &= 1, \\ \alpha_{SP1} + \alpha_{SP2} &= 0, \end{aligned} \quad (17)$$

we determine  $\alpha_{Skr}$  as

$$\begin{aligned} \alpha_{SP1} &= -\frac{(\rho_{SS} + \omega_1)(\rho_{SS} + \omega_2)}{\rho_{PS}(\omega_2 - \omega_1)}, & \alpha_{SS1} &= \frac{\rho_{SS} + \omega_2}{\omega_2 - \omega_1}, \\ \alpha_{SP2} &= \frac{(\rho_{SS} + \omega_1)(\rho_{SS} + \omega_2)}{\rho_{PS}(\omega_2 - \omega_1)}, & \alpha_{SS2} &= -\frac{\rho_{SS} + \omega_1}{\omega_2 - \omega_1}. \end{aligned} \quad (18)$$

Putting expressions in (13), (16), and (18) together, we get

$$\begin{aligned}\mathcal{P}_{PP}(t - \kappa) &= \frac{\rho_{PP} + \omega_2}{\omega_2 - \omega_1} e^{-\omega_1(t - \kappa)} - \frac{\rho_{PP} + \omega_1}{\omega_2 - \omega_1} e^{-\omega_2(t - \kappa)}, \\ \mathcal{P}_{SS}(t - \kappa) &= \frac{\rho_{SS} + \omega_2}{\omega_2 - \omega_1} e^{-\omega_1(t - \kappa)} - \frac{\rho_{SS} + \omega_1}{\omega_2 - \omega_1} e^{-\omega_2(t - \kappa)}, \\ \mathcal{P}_{PS}(t - \kappa) &= \frac{(\rho_{PP} + \omega_1)(\rho_{PP} + \omega_2)}{\rho_{SP}(\omega_2 - \omega_1)} \left( e^{-\omega_2(t - \kappa)} - e^{-\omega_1(t - \kappa)} \right), \\ \mathcal{P}_{SP}(t - \kappa) &= \frac{(\rho_{SS} + \omega_1)(\rho_{SS} + \omega_2)}{\rho_{PS}(\omega_2 - \omega_1)} \left( e^{-\omega_2(t - \kappa)} - e^{-\omega_1(t - \kappa)} \right).\end{aligned}\tag{19}$$

The remaining transition probabilities,  $\mathcal{P}_{PI}$  and  $\mathcal{P}_{SI}$ , in the full three-state model are determined from the facts that  $\mathcal{P}_{PI} = 1 - \mathcal{P}_{PP} - \mathcal{P}_{PS}$  and  $\mathcal{P}_{SI} = 1 - \mathcal{P}_{SP} - \mathcal{P}_{SS}$ . Note, that the term '1' corresponds to the zero eigenvalue of a  $3 \times 3$  matrix  $\mathbf{G}$ .

Our next step is a discussion of survivability, which will incorporate the transition probabilities derived above in (19), as well as the expected value needed to derive the rate of infection from the initially susceptible partner.

### 3.3.3. **Prob 5: survival function and expected value**

Finally we compute **Prob 5**, the probability that initially susceptible partner  $Y$  becomes infected at time  $t$ , while being in group  $j \in P, S$ . Since we have two uninfected groups,  $S$  and  $P$ , an individual  $Y$  may transition between the two groups before becoming infected. This probability is the product of being a partner after  $\tilde{t}$  years and the probability of not getting infected within  $\tilde{t}$  years of the start of a long-term partnership. If the probability of remaining in the partnership is represented by an exponential random variable with mean  $\tau$ , as in **Prob 2**, then we denote

$$S_{jk}(t - \kappa) = e^{-\frac{(t-\kappa)}{\tau}} \cdot \mathcal{P}_{jk}(t - \kappa),\tag{20}$$

where  $S_{jk}(t - \kappa)$  indicates that the long-term partner  $Y$  was in state  $j$  at time  $\kappa$  and in state  $k$  at time  $t$  [55] and with transition probabilities  $\mathcal{P}_{jk}(\tilde{t})$  obtained in (19). The expected value is then defined to be

$$E[I^{new}(t - \kappa)] \equiv \int_{\Omega} g(u)f(u) du,\tag{21}$$

with

$$g_{jk}(t - \kappa) = \begin{cases} P(\kappa)\rho_{kI}(t - \kappa), & k = P \\ S(\kappa)\rho_{kI}(t - \kappa), & k = S, \end{cases}$$

where  $\rho_{kI}$  is a transition hazard from state  $k$  to infected group  $I$ , and  $f(\cdot)$  denotes a probability density function related to  $\mathcal{S}$  through identity  $-f = \frac{d}{dt}\mathcal{S}$ .

### 3.3.4. **Combining Prob 3–Prob 5 to calculate $\lambda_p^{S/P}$**

Now we can use the functions (20) to derive the corresponding probability density functions and, combined with the appropriate transition hazards ( $\rho_{jk}$  in (10)), apply them in the integral definition of the expected value (21) to determine the expressions for the rates of infection in all four scenarios:

(1) **Individual Y is in S at the start of the long-term relationship  $\kappa$  as well as at the time of infection  $t$**

The probability density function

$$\begin{aligned} f(\tilde{t}) &= -\frac{d}{d(\tilde{t})} \left[ e^{-\frac{\tilde{t}}{\tau}} \cdot \mathcal{P}_{SS}(\tilde{t}) \right] \\ &= \frac{1}{(\omega_1 - \omega_2)\tau} e^{-\frac{\tilde{t}}{\tau}} \left[ (\rho_{SS} + \omega_1)(1 + \omega_2\tau) e^{-\omega_2\tilde{t}} - (\rho_{SS} + \omega_2) \right. \\ &\quad \left. \times (1 + \omega_1\tau) e^{-\omega_1\tilde{t}} \right], \end{aligned} \quad (22)$$

is used in calculation of the rate of infection

$$\lambda_p^{SS} = \psi \int_0^\infty g_{SS}(\tilde{t})f(\tilde{t}) d\tilde{t} = \int_0^\infty \psi \bar{\lambda} \xi \tilde{t} S(\kappa) \cdot f(\tilde{t}) d\tilde{t}. \quad (23)$$

(2) **Individual Y is in P at the start of the long-term relationship ( $\kappa$ ) but stops PrEP and transitions to S, and remains there at the time of infection  $t$**

The probability density function

$$\begin{aligned} f(\tilde{t}) &= -\frac{d}{d(\tilde{t})} \left[ e^{-\frac{\tilde{t}}{\tau}} \cdot \mathcal{P}_{PS}(\tilde{t}) \right] \\ &= \frac{(\rho_P + \omega_1)(\rho_P + \omega_2)}{(\omega_1 - \omega_2)\rho_{SP}\tau} e^{-\frac{\tilde{t}}{\tau}} \left[ (1 + \omega_1\tau) e^{-\omega_1\tilde{t}} - (1 + \omega_2\tau) e^{-\omega_2\tilde{t}} \right], \end{aligned} \quad (24)$$

is used in a calculation of the rate of infection

$$\lambda_p^{PS} = \psi \int_0^\infty g_{PS}(\tilde{t})f(\tilde{t}) d\tilde{t} = \int_0^\infty \psi \bar{\lambda} \xi \tilde{t} P(\kappa) \cdot f(\tilde{t}) d\tilde{t}. \quad (25)$$

(3) **Individual Y is in P at the start of the long-term relationship ( $\kappa$ ) as well as at the time of infection ( $t$ )**

The probability density function

$$\begin{aligned} f(\tilde{t}) &= -\frac{d}{d(\tilde{t})} \left[ e^{-\frac{\tilde{t}}{\tau}} \cdot \mathcal{P}_{PP}(\tilde{t}) \right] \\ &= \frac{1}{(\omega_1 - \omega_2)\tau} e^{-\frac{\tilde{t}}{\tau}} \left[ (\rho_P + \omega_1)(1 + \omega_2\tau) e^{-\omega_2\tilde{t}} - (\rho_P + \omega_2)(1 + \omega_1\tau) \right. \\ &\quad \left. \times e^{-\omega_1\tilde{t}} \right], \end{aligned} \quad (26)$$

is used in a calculation of the rate of infection

$$\lambda_p^{PP} = \psi \int_0^\infty g_{PP}(\tilde{t})f(\tilde{t}) d\tilde{t} = \int_0^\infty \psi \bar{\lambda} \xi (1 - qr) \tilde{t} v(\kappa) \cdot f(\tilde{t}) d\tilde{t}. \quad (27)$$

(4) **Individual Y is in S at the start of the long-term relationship ( $\kappa$ ) but starts PrEP and transitions to P, and remains there at the time of infection ( $t$ )**

The probability density function

$$\begin{aligned} f(\tilde{t}) &= -\frac{d}{d(\tilde{t})} \left[ e^{-\frac{(\tilde{t})}{\tau}} \cdot \mathcal{P}_{SP}(\tilde{t}) \right] \\ &= \frac{(\rho_{SS} + \omega_1)(\rho_{SS} + \omega_2)}{(\omega_1 - \omega_2)\rho_{PS}\tau} e^{-\frac{\tilde{t}}{\tau}} \left[ (1 + \omega_1\tau) e^{-\omega_1\tilde{t}} - (1 + \omega_2\tau) e^{-\omega_2\tilde{t}} \right], \end{aligned} \quad (28)$$

is used in a calculation of the rate of infection

$$\lambda_p^{SP} = \psi \int_0^\infty g_{SP}(\tilde{t})f(\tilde{t}) d\tilde{t} = \int_0^\infty \psi \bar{\lambda} \xi (1 - qr) \tilde{t} s(\kappa) \cdot f(\tilde{t}) d\tilde{t}. \quad (29)$$

We combine the four scenarios to obtain the total rate of infection from initially susceptible partner in either  $P$  or  $S$  as

$$\begin{aligned} \lambda_p^{S/P} &= \lambda_p^{SS} + \lambda_p^{SP} + \lambda_p^{PP} + \lambda_p^{PS} \\ &= \frac{\psi \bar{\lambda} \xi}{(\omega_1 - \omega_2)\rho_{SP}\rho_{PS}\tau} \int_0^\infty e^{-\frac{1}{\tau}\tilde{t}} \left\{ e^{-\omega_1\tilde{t}}(1 + \omega_1\tau)\Upsilon_{12} - e^{-\omega_2\tilde{t}}(1 + \omega_2\tau)\Upsilon_{21} \right\} \tilde{t} d\tilde{t}, \end{aligned}$$

where

$$\begin{aligned} \Upsilon_{jk} &= \rho_{SP}(\omega_k + \rho_{SS})[(\omega_j + \rho_{SS})(1 - qr) - \rho_{PS}]S(\kappa) + \\ &\quad + \rho_{PS}(\omega_k + \rho_{PP})[\omega_j + \rho_{PP} - \rho_{SP}(1 - qr)]P(\kappa). \end{aligned}$$

Using the linear approximations of  $P(\kappa)$  and  $S(\kappa)$ :

$$\begin{aligned} P(\kappa) &\approx P(t) + (\kappa - t)[\mu\alpha + \theta S(t) - (1 - qr)\bar{\lambda}P(t) - (\sigma + \mu)P(t)] \\ &= -\mu\alpha\tilde{t} - \theta\tilde{t}S(t) + P(t)[1 + (\sigma + \mu + \bar{\lambda}(1 - qr))\tilde{t}], \\ S(\kappa) &\approx S(t) + (\kappa - t)[\mu(1 - \alpha) + \sigma P(t) - \bar{\lambda}S(t) - (\theta + \mu)S(t)] \\ &= -\mu(1 - \alpha)\tilde{t} - \sigma P(t)\tilde{t} + S(t)[1 + (\bar{\lambda} + \theta + \mu)\tilde{t}], \end{aligned} \quad (30)$$

and evaluating the integral with the help of Mathematica, we get

$$\lambda_p^{S/P} = \psi \cdot F(\bar{\lambda}\tau\xi, t),$$

where

$$\begin{aligned} F(\bar{\lambda}\tau\xi, t) &= \frac{\bar{\lambda}\xi\tau}{C} \left\{ -2\mu\tau (1 - qr\alpha + B\tau[2 + \tau(B + qr(\theta + \alpha\bar{\lambda}\xi))]) \right. \\ &\quad \left. + S(t)(1 + \tau(A + 2B + 3\theta qr) + B\tau^2(2A + B + \theta qr) \right. \\ &\quad \left. + B\tau^3[(A + \bar{\lambda}\xi)\theta qr + AB]) \right\} \end{aligned}$$

$$\begin{aligned}
& + P(t) ((1 - qr)(1 + \tau[A + 2B + (2\theta - \bar{\lambda}\xi - 2\sigma)qr]) - \sigma\tau qr) \\
& + P(t) (B\tau^2[2A + B + qr(\theta - 4\bar{\lambda} - \bar{\lambda}\xi)]) \\
& + B\tau^3[AB + 2qr[\mu(\theta + \bar{\lambda}\xi) - \sigma\bar{\lambda} + \sigma\bar{\lambda}\xi])\}, \\
A & = 2\mu + 2\bar{\lambda} + \bar{\lambda}\xi, \\
B & = \sigma + (1 - qr)(\theta + \bar{\lambda}\xi), \\
C & = [(\theta\tau + 1 + \bar{\lambda}\xi\tau)(1 + \bar{\lambda}\xi\tau(1 - qr)) + \sigma\tau(1 + \bar{\lambda}\xi\tau)]^2.
\end{aligned}$$

Now, the linear approximation around  $\bar{\lambda} = 0$ ,

$$\begin{aligned}
F(\bar{\lambda}\tau\xi, t) & \approx F(0, t) + \left. \frac{\partial F}{\partial \bar{\lambda}} \right|_{\bar{\lambda}=0} \cdot (\bar{\lambda} - 0) \\
& = \frac{\bar{\lambda}\tau\xi}{(1 + \theta\tau + \sigma\tau)^2} \{ -2\mu\tau[(1 + \theta\tau + \sigma\tau)^2 - qr(\alpha + \theta\tau(2 + \theta\tau + \sigma\tau))] \\
& + [1 + 2\tau(\theta + \mu + \sigma)][S(t) + (1 - qr)P(t)] + \tau qr[\theta S(t) - \sigma P(t)] \\
& + \tau^2[\theta(1 - qr) + \sigma][(\theta + \sigma)(1 + 2\mu\tau) + 4\mu][S(t) + P(t)] \},
\end{aligned}$$

and hence the rate of infection from a partner acquired while susceptible is calculated to be

$$\begin{aligned}
\lambda_p^{S/P} & \equiv \psi E[I^{new}] \\
& \approx \frac{\psi\bar{\lambda}\tau\xi}{(1 + \theta\tau + \sigma\tau)^2} \{ -2\mu\tau[(1 + \theta\tau + \sigma\tau)^2 - qr(\alpha + \theta\tau(2 + \theta\tau + \sigma\tau))] \\
& + [1 + 2\tau(\theta + \mu + \sigma)][S(t) + (1 - qr)P(t)] + \tau qr[\theta S(t) - \sigma P(t)] \\
& + \tau^2[\theta(1 - qr) + \sigma][(\theta + \sigma)(1 + 2\mu\tau) + 4\mu][S(t) + P(t)] \}. \quad (31)
\end{aligned}$$

### 3.4. Rate of infection from all partnership models: $\lambda = \lambda_z + \lambda_p^I + \lambda_p^{S/P}$

Our full model considers casual as well as long-term partnerships with both infected and initially susceptible individuals. Therefore we can describe the rate of infection as  $\lambda = \lambda_z + \lambda_p^I + \lambda_p^{S/P}$ . Using the expressions obtained previously, and solving the resulting equation explicitly, we obtain the rate of infection for the most comprehensive non-monogamous long-term case of *PSI* model,

$$\lambda = \frac{(\mathcal{K} + \mathcal{L}S + \mathcal{M}P)I}{\mathcal{D}^2\{1 + \chi\tau[S + (1 - qr)P]\}}, \quad (32)$$

where

$$\begin{aligned}\mathcal{D} &= 1 + \theta\tau + \sigma\tau, \\ \mathcal{N} &= \mathcal{D}^2 - qr\theta\tau(\mathcal{D} + 1), \\ \mathcal{K} &= \mathcal{D}^2[z\beta + \chi(1 + \mu\tau)] - 2\bar{z}\beta\zeta\mu\tau^2\psi(\mathcal{N} - qra), \\ \mathcal{L} &= \beta\tau\{\mathcal{D}^2z\chi + \bar{z}\zeta\psi[\mathcal{N}(1 + 2\mu\tau) + 3qr\theta\tau]\}, \\ \mathcal{M} &= \beta\tau\{\mathcal{D}^2(1 - qr)z\chi + \bar{z}\zeta\psi[(1 + 2\mu\tau)(\mathcal{N} - qr) - 3qr\sigma\tau]\}.\end{aligned}\quad (33)$$

### 3.5. Reproduction number and disease-free equilibrium

The reproduction number is calculated using the next-generation method and expressed as

$$\mathcal{R} = \frac{[\mathcal{K}\mathcal{T} + \mathcal{L}(\mu(1 - \alpha) + \sigma) + \mathcal{M}(\theta + \mu\alpha)][\mathcal{T} - qr(\theta + \mu\alpha)]}{\mathcal{D}^2\mu\mathcal{T}[\mathcal{T}(1 + \chi\tau) - qr\chi\tau(\theta + \mu\alpha)]}, \quad (34)$$

with  $\mathcal{T} = (\mu + \theta + \sigma)$  and the other parameters are given in Equation (33). The disease-free equilibrium (DFE) is,

$$(P^*, S^*, I^*) = \left( \frac{\theta + \alpha\mu}{\sigma + \mu + \theta}, \frac{\sigma + \mu - \alpha\mu}{\sigma + \mu + \theta}, 0 \right). \quad (35)$$

We establish the local stability of the DFE by analysing the eigenvalues of the Jacobian for the system (1), with the rate of infection (32). The associated characteristic equation, evaluated at the DFE (35), is given by

$$p(\lambda) = \begin{vmatrix} -\mu - \sigma - \lambda & \theta & -\mathcal{J}(1 - qr)(\theta + \mu\alpha) \\ \sigma & -\mu - \theta - \lambda & -\mathcal{J}[\mu(1 - \alpha) + \sigma] \\ 0 & 0 & \mathcal{J}[\mathcal{T} - qr(\theta + \mu\alpha)] - \mu - \lambda \end{vmatrix}, \quad (36)$$

where

$$\mathcal{J} = \frac{\mathcal{K}\mathcal{T} + \mathcal{L}(\mu(1 - \alpha) + \sigma) + \mathcal{M}(\theta + \mu\alpha)}{\mathcal{D}^2\mathcal{T}[\mathcal{T}(1 + \chi\tau) - qr\chi\tau(\theta + \mu\alpha)]}.$$

The three real zeros of  $p(\lambda)$  are the eigenvalues of the Jacobian. The first two,  $\lambda_1 = -\mu$ ,  $\lambda_2 = -\mathcal{T} = -(\mu + \theta + \sigma)$ , are always negative and the third one, simplified to  $\lambda_3 = \mu(\mathcal{R} - 1)$ , is negative only when previously calculated reproduction number (34) satisfies  $\mathcal{R} < 1$ . We therefore conclude the classic result from Castillo-Chavez [56] that DFE is locally asymptotically stable when the reproductive number  $\mathcal{R} < 1$  and unstable when  $\mathcal{R} > 1$ .

## 4. Estimating parameter values

We define the number of long-term partners per year,  $p/\tau$ , from pair formation models. Using the definitions reviewed in [30],  $M$  is the number of lifetime long-term partners, and  $M = f/(\mu(f\tau + 1))$ , where  $f$  is the pair formation rate,  $\tau$  is the partnership duration, and  $1/\mu$  is the lifetime. So the number of long-term partners per year is  $M\mu = f/(1 + f\tau)$ ,

which is our definition for  $p/\tau$  [33]. In [33] it was shown that with these definitions, the long-term partnership model matches the behaviour of the pair formation model with both reproduction numbers and numerical simulations in time.

We assume that the total population is constant with the recruitment rate equal to the population removal rate  $\mu = 1/61$ , as stated in Table 1. We start our numerical simulations assuming that 1% of the individuals entering the population of sexually active MSM are already using PrEP. We must keep in mind that, as of 2023, PrEP prescriptions have only been recommended to HIV-negative and sexually active individuals who are at the high risk of infection. However, in the study [27], nearly 40% of those currently using PrEP did not meet these indications for PrEP, and 68% of MSM who met the indications for PrEP were not currently using PrEP. Hence, we introduce in our models the parameter  $\alpha$  to explore the possible benefits of administering PrEP as a preemptive measure to those who have not been exposed to the virus, yet. We choose  $\alpha = 0.01$  to indicate the fraction of individuals who begin PrEP treatment before becoming sexually active and entering the susceptible population.

Nationwide data on PrEP initiation and persistence are very limited. When choosing the baseline values for the parameters related to PrEP use, we relied on the CDC reports [3] and on the published findings based on various studies and PrEP trials in different parts of the world. In their 2019 surveillance report, the CDC stated that approximately 25% of the roughly 0.8 million eligible MSM have started PrEP, which represents only 3% of the estimated number of MSM in the United States. A similar estimate was given in 2020 by Koss et al. [57], who did an interim analysis of observational data from the ongoing SEARCH (Sustainable East Africa Research in Community Health) study and noted that only one-quarter of the individuals assessed as being at elevated risk initiated PrEP within 90 days, with even lower initiation among young adults. In 2016, Parsons et al. [58] analysed data from 995 men in One Thousand Strong, a longitudinal study of a national panel of HIV-negative gay and bisexual men in the United States, and found that a large majority of participants were appropriate candidates for PrEP, yet fewer than 1 in 10 were using PrEP. On the other hand, Dean et al. [44] analysed PrEP pharmacy claims and HIV diagnoses from a Symphony Health Solutions dataset across all U.S. states from October 1, 2015 to September 30, 2019, and calculated the percentage of individuals, who were newly prescribed PrEP but either reversed, delayed, or abandoned it in the next 365 days, to be about 17%. Our chosen baseline values of  $\theta = 0.05$  and  $\sigma = 0.2$  are consistent with the literature and correspond to having 5% of all the susceptible individuals initiate PrEP, with 20% of them suspending it within a year.

Data from trials, open-label extension studies, and demonstration studies have shown that oral PrEP is effective in preventing HIV infection in cisgender men who have sex with men, and, when used consistently, it may reduce the risk of infection by up to 99% [11, 12]. This brings up an important aspect to consider, namely PrEP adherence. It is rather common knowledge that greater adherence is associated with greater efficacy of PrEP. Nevertheless, the levels of adherence with daily dosages vary greatly across different regions, age groups of patients, and their race or economic status. In 2019, Chou et al. [59] published a PrEP initiation and adherence review of previously conducted studies. Three observational studies of adult U.S. men who have sex with men found adherence to PrEP to be 66% to 90%, based on the level of tenofovir in dried blood sampling (consistent with 4 doses per week). Using the same measure, two observational studies of younger U.S. men

who have sex with men found adherence to PrEP of approximately 50% at 12 weeks and 22% to 34% at 48 weeks. A randomized controlled clinical trial of primarily (97%) U.S. men who have sex with men found that adherence was higher with daily (48%) than with intermittent (31%) or event-driven (17%) PrEP during weeks in which sex was reported. Based on their analysis of a study in East Africa, Koss et al. [57] concluded that one-third of participants reporting HIV risk and adherence during follow-up had concentrations of tenofovir in their hair that were consistent with poor adherence (fewer than four PrEP doses per week). Using the results published in literature we assume a 50% adherence and set the corresponding parameter  $q = 0.5$  as our baseline value.

We calculate our  $\beta$ , the estimates of per-act HIV transmission risks from an infected source to an HIV-uninfected person through various means of exposure through sexual activity, using the parameters in the supplemental digital content, Technical Report for the HIV Optimization and Prevention Economics (HOPE) Model, June 2021 of [47]. The HOPE programme is a differential equations model representing the U.S. HIV epidemic developed by the CDC's Division of HIV/AIDS Prevention and RTI International (an independent non-profit research institute). We use the HOPE data for the first time period, 2010 to 2018, to replicate historical data and trends in the United States. The values  $b_i$  and  $b_r$  represent the per-act HIV transmission risk for insertive and receptive MSM, respectively, and were determined by a data fit. The CDC reported that in 2015 58% of the U.S. HIV<sup>+</sup> were virally suppressed [60]. Thus in this model, we assume that 60% of the HIV<sup>+</sup> is virally suppressed. We define  $\beta = (.4 \times \beta_{chronic} + .6 \times \beta_{viralsuppressed})$ ,  $\beta_{chronic} = 1/2(b_i + b_r)$  where  $b_i$  is transmission rate per insertive act and  $b_r$  is transmission rate per receptive act when partner is chronically infected and  $\beta_{viralsuppressed} = 0.06\beta_{chronic}$  [61].

Although the underlying drivers of HIV transmission among MSM may vary based on main (long-term) and casual partner types, little is known about the change in the number and composition of sex partner types nationally, and, thus, which relationship contexts should be prioritized for HIV prevention. Rosenberg et al. [28] analysed data from the first MSM cycle of the CDC National HIV Behavioral Surveillance system, conducted from 2003 to 2005, and concluded that among 11,191 sexually active MSM, 32% reported having only male casual partners, 44% had long-term (main) and casual partners, and 24% had long-term (main) partners exclusively. Those who had no long-term male partners during the previous year had a median of 5 casual male partners, while those with a long-term male partner had a median of 2 casual male partners. The updated results were published by Chapin-Bardales et al. [29], who used CDC's National HIV Behavioral Surveillance data from 2008, 2011, and 2014, to study trends in the number and partner type composition (long-term/casual) of male sex partners among 28,061 U.S. MSM. According to their reports, the adjusted mean total number of male sex partners in the past 12 months increased among MSM to 7.7 in 2014. Since we are trying to capture the results from 2005-2025 we use the HOPE data study [47] for 2005-2018 attributing the average number of casual partners per year as  $z = 6.1$ , a number in the middle of these different studies. We define  $\bar{z} = 2$ , average number of casual partners outside of long-term partnership, again consistent with the above findings. By the HOPE data, the number of sexual acts per year is 68, so we set  $n = 68\tau$  where  $n$  is the number of sexual acts over the duration of long-term partnership.

## 5. Comparison of our model to CDC data

Since we determined our parameter values using reported data for the U.S., but not by fitting to the U.S. HIV data as reported by the CDC, we can compare the model results to the CDC measurements to test the validity of the predictive power of our model. The initial conditions for the simulations correspond to the data reported by the CDC [62] in 2005 with 9% of the MSM population infected with HIV. Figure 3 shows the incidence of new infections and prevalence of HIV infections each year from 2005 to 2020 for MSM in the U.S. with both long-term and casual partnerships included in the model along with CDC incidence and prevalence data. The incidence and prevalence data from the CDC HIV Surveillance reports, HIV Surveillance Supplemental Reports, and prior to 2008 the HIV/AIDS Surveillance reports [63] are shown using the blue circles. Data for each year represents the multiple years that the CDC updates its data estimates, hence the multiple data points for some years. The solid red curve is a curve fit to CDC data and the green dashed lines represent a 95% confidence interval for the data. The black dashed line in the prevalence graph Figure 3(a) represents the model output for prevalence. The model output for incidence was created by fitting the model prevalence output to a quadratic curve (this curve is not shown in Figure 3(a)). The slope of the quadratic curve at evaluated at year intervals represents the HIV incidence for that year and is illustrated in Figure 3(b) by the dashed black line. Figure 3 illustrates that our model closely approximates the incidence and prevalence of HIV infections in the U.S. in from the 2005-2019 data with our parameters as given in Table 1. The model is primarily within the 95% confidence interval for HIV prevalence in MSM and it stays entirely within the 95% confidence interval for the incidence. Figure 4 shows the percentage of HIV negative MSM individuals in the U.S. taking PrEP. Note that these dots are not aligned with the CDC previous definition of coverage. The blue dots correspond to CDC data as reported by [64-66]. For the initial 2012 data point, the CDC reported [64] that 1.2 million persons of the U.S. population fit

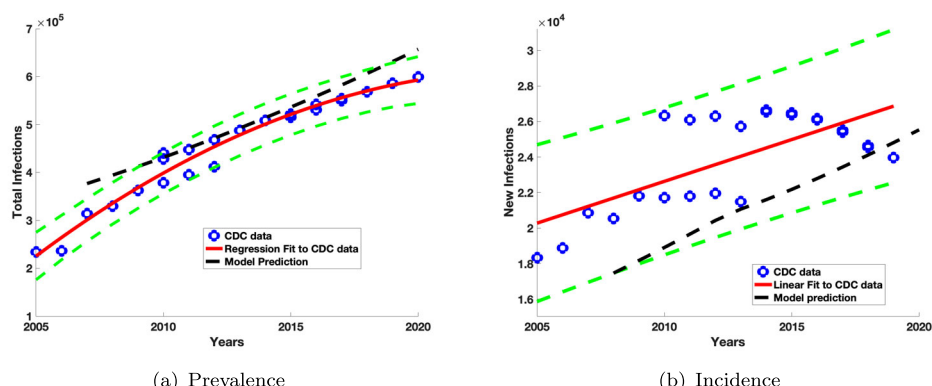


**Figure 3.** The HIV incidence and prevalence are plotted as a function of the year between 2005 and 2020 for the model that includes both casual and long-term partnerships. The blue dots are data from the CDC. The black dashed line corresponds to the model output and the solid red curve corresponds to the linear (Incidence) and quadratic (Prevalence) regression that fits the CDC data over this time interval. The green dashed curves correspond to the 95% confidence interval. This model starts in 2007 and PrEP usage began in 2012.

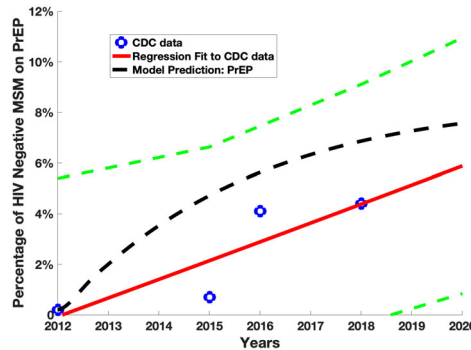


**Figure 4.** The blue dots represent data from the MSM HIV negative men on PrEP from the CDC. The black dashed line corresponds to model output and the solid red curve corresponds to the linear regression fits to the CDC data over this time interval. The green dashed curves correspond to the 90% confidence interval.

the risk category for PrEP, but only 0.7% of those indicated took PrEP. AIDSVu.org also stated that 93% of the recommended population was male, although the sexual behaviour of the gender was not recorded. We do not include CDC coverage information for ‘the proportion of MSM with indications who start PrEP’ for two reasons. First, in the study [27] nearly 40% of those currently using PrEP did not meet these indications for PrEP, and 68% of MSM who met the indications for PrEP were not currently using PrEP. Hence, we did not divide our populations between high and low risk. Second, as of 2024, the CDC has paused PrEP coverage reporting to determine the best methodology for calculating PrEP coverage. Coverage reporting will be resumed in June 2025 with updated PrEP coverage estimates using updated methods and sources [15]. The solid red curve in Figure 4 is a curve fit to CDC data and the green dashed lines represent a 90% confidence interval for the data. The black dashed line in the prevalence graph Figure 3(a) represents the model output for prevalence. Figure 4 illustrates that our model approximates the percentage of HIV negative MSM taking PrEP and stays well within the 90% confidence interval.

## 6. Analysis of PrEP parameters on the reproduction number

The reproduction number of the model, given by Equation (34), has complex dependence on the parameter values. In this section, we analyse how the reproduction number depends on the PrEP parameters  $\sigma, \theta, q$ . Our model assumes that PrEP parameters  $\sigma, \theta, q$  vary continuously. The figures below illustrate how the impact to the reproduction number of changing the baseline parameters of  $\sigma = 0.2, q = 0.5$ , and  $\theta = 0.05$  by increasing  $q$  and  $\theta$  and decreasing  $\sigma$ . We do not include studies with the parameter  $\alpha$ , the proportion of people starting PrEP as they become sexually active since even  $\alpha = 1$  changes the reproduction number by less than 0.1.

Figure 5(a) shows contour plots of the reproduction number  $\mathcal{R}$  plotted as functions of  $\theta$  and  $q$ , as  $\sigma$  decreases from 0.2 to 0.05. The thick black line in the plots correspond to  $\mathcal{R} = 1$  with the blue colours above the  $\mathcal{R} = 1$  line corresponding to  $\mathcal{R} < 1$  and the red colours below the  $\mathcal{R} = 1$  line corresponding to  $\mathcal{R} > 1$ . First note the change in the plots as  $\sigma$  decreases from 0.2 to 0.05. Decreasing  $\sigma$  from 0.2 to 0.1 produces a larger shift in the

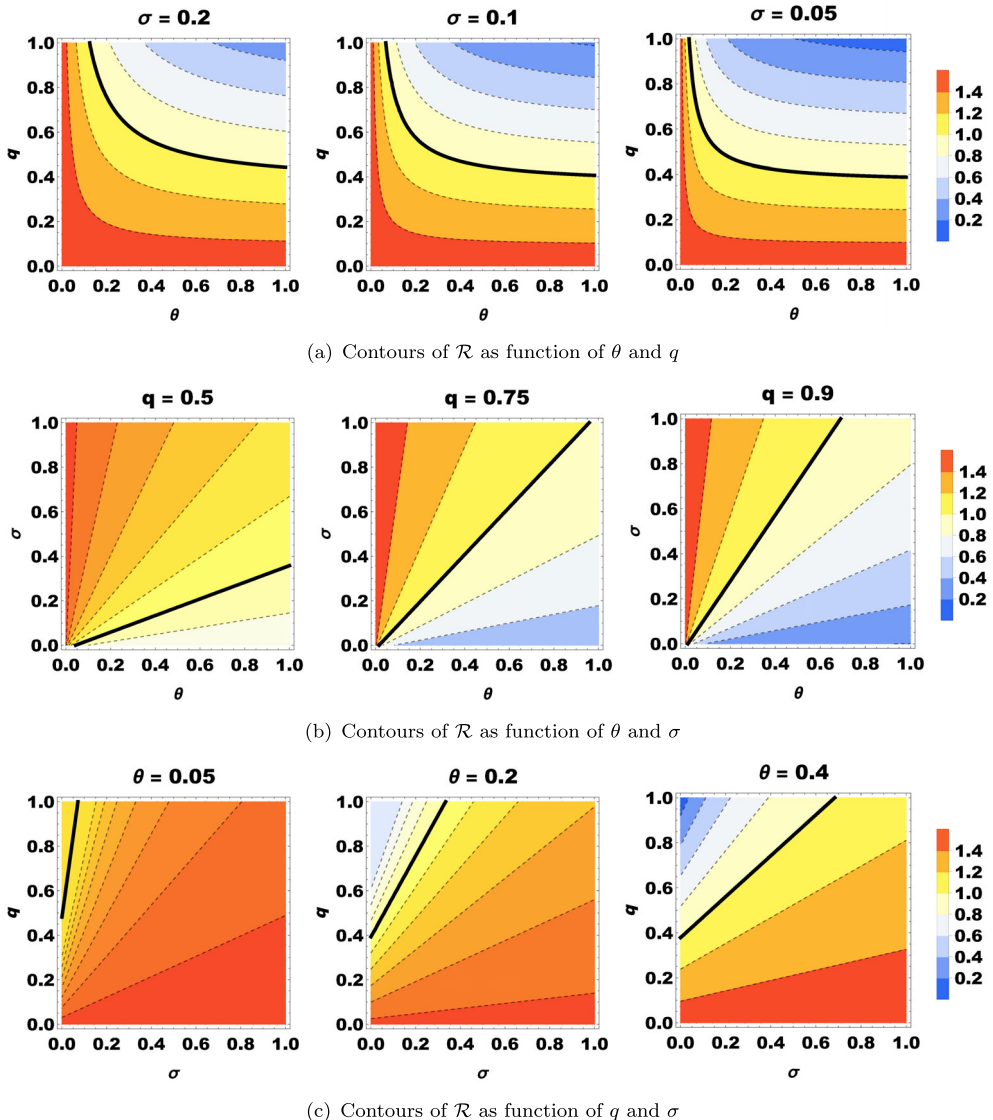


**Figure 5.** Contours of reproduction number  $\mathcal{R}$ . (a) Row 1 shows  $\mathcal{R}$  plotted as a function of  $\theta$ , the rate of starting PrEP, and  $q$ , the level of adherence, assuming the baseline parameter values listed in Table 1. (b) Row 2 shows  $\mathcal{R}$  plotted as a function of  $\theta$ , the rate of starting PrEP, and  $\sigma$ , the treatment discontinuation rate. (c) Row 3 shows  $\mathcal{R}$  plotted as a function of  $q$ , the level of adherence, and  $\sigma$ , rate of discontinuation. The contour for  $\mathcal{R} = 1$  is the thick black curve in all subfigures.

$\mathcal{R} = 1$  line than the shift from decreasing  $\sigma$  from 0.1 to 0.05. For values of  $\theta$  larger than about 0.3, the required adherence is around 40-50%.

Figure 5(b) illustrates contour plots of reproduction numbers, similar to Figure 5(a) except the contours are a function of  $\theta$  and  $\sigma$  for three values of  $q$ . Below the  $\mathcal{R} = 1$  line corresponds to  $\mathcal{R} < 1$  and above the  $\mathcal{R} = 1$  line corresponds to  $\mathcal{R} > 1$ . Note that increasing the adherence from 0.5 to 0.75 significantly changes the contours with the higher adherence

having a much larger region that corresponds to  $\mathcal{R} < 1$ . A 50% adherence  $q = 0.5$  requires that for  $\sigma = 0.1$ ,  $\theta$  is approximately 0.5 to achieve a reproduction number less than one. However, for  $q = 0.75$  and  $\sigma = 0.1$ , a value of  $\theta \approx 0.2$  can achieve the same result. Increasing the adherence from 0.75 to 0.9 does not change the  $\mathcal{R} = 1$  contour as significantly as the previously described increase in adherence.

Finally, in Figure 5(c), we illustrate three contour plots of  $\sigma$  vs  $q$  as  $\theta$  varies from the baseline value of 0.05 to 0.4. In this plot the region above the  $\mathcal{R} = 1$  contour line corresponds to  $\mathcal{R} < 1$  and the region below the  $\mathcal{R} = 1$  contour line corresponds to  $\mathcal{R} > 1$ . For the baseline value of  $\theta = 0.05$ , the  $\mathcal{R} < 1$  region is so small, that disease elimination is almost impossible. For  $\theta = 0.2$  the size of the region corresponding to  $\mathcal{R} < 1$  increases but still requires unachievable values of  $\sigma$  and  $q$ . For  $\theta = 0.4$ , the size of the  $\mathcal{R} < 1$  region increases, but still requires an adherence of at least 0.4. As suggested by the previous two figures, we increase the likelihood of achieving  $\mathcal{R} < 1$  by decreasing  $\sigma$  to 0.1 and increasing the adherence to 0.75. For these two values of discontinuation rate and adherence, we would need  $\theta$  to be at least 0.2, which is four times the current estimate.

## 7. Sensitivity analysis of PrEP parameters

Sensitivity analysis is necessary to explore the dynamics of the epidemiological models because their structural complexity comes with a high degree of uncertainty in estimating the values of many of the input parameters. A sensitivity analysis can identify which input parameters are important (due to their estimation uncertainty) in contributing to the prediction imprecision of the outcome variable [67]. Knowledge of the relative importance of the different factors responsible for transmission is useful to determine the best control measures. Initially disease transmission is related to reproduction number  $\mathcal{R}$  and sensitivity predicts which parameters have a high impact on its value.

To consider the implications of our model in a more comprehensive manner, in this section we conduct global uncertainty and sensitivity analysis through Latin Hypercube Sampling (LHS) and Partial Rank Correlation Coefficients (PRCC) for the three parameters of the rate of starting PrEP, the rate of stopping PrEP, and the adherence rate to the daily regime. The sign of the PRCC indicates the qualitative relationship between each input variable and each output variable. The magnitude of the PRCC indicates the importance of the uncertainty in estimating the value of the input variable in contributing to the imprecision in predicting the value of the outcome variable. The relative importance of the input variables can be directly evaluated by comparing the values of the PRCC as a first step in assessing the global sensitivity of a model on the uncertainties in its parameters. In Figure 6, we can see that the reproduction number is globally sensitive to uncertainty in the values of  $\theta$ ,  $\sigma$ , and  $q$ . However, the PRCC calculation does not capture the full story. Thus, in this section, we use additional sensitivity measures to describe the sensitivity of the reproduction number to the level of adherence, and rate of initiating and stopping PrEP.

The sensitivity index of  $\mathcal{R}$  with respect to a parameter  $\omega$  is  $\frac{\partial \mathcal{R}}{\partial \omega}$ . Another measure is the elasticity index (normalized sensitivity index) that measures the relative change of  $\mathcal{R}$  with respect to  $\omega$ , denoted by  $\mathcal{F}_\omega^{\mathcal{R}}$ , and defined as

$$\mathcal{F}_\omega^{\mathcal{R}} = \frac{\partial \mathcal{R}}{\partial \omega} \times \frac{\omega}{\mathcal{R}}.$$

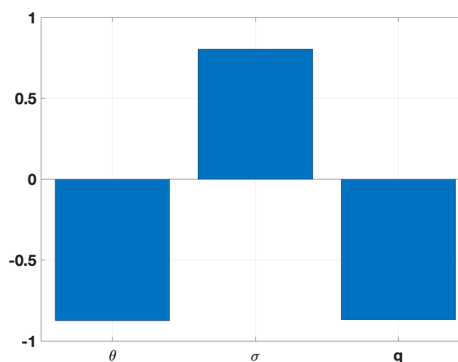


**Figure 6.** PRCC values for control parameters as a function of the reproduction number.

Each elasticity index value can be interpreted as the effective change in the reproduction number with respect to the applied change in the given parameter. For example, an elasticity index of 0.3 means that for every 10% increase in  $\omega$ , the reproduction number will increase by 3%. The sign of the elasticity index specifies whether  $\mathcal{R}$  increases (positive sign) or decreases (negative sign) with the parameter; whereas the magnitude determines the relative importance of the parameter. If  $\mathcal{R}$  is known explicitly, then the elasticity index for each parameter can be computed explicitly, and evaluated for a given set of parameters. The magnitude of the elasticity indices depends on these parameter values, which are often only estimates.

For our model, we will start by calculating elasticity indices of the 3 control parameters associated with PrEP: the rate of initiating PrEP,  $\theta$ , rate of suspending PrEP,  $\sigma$ , and the level of adherence to daily PrEP regimen,  $q$ . We use previously calculated expressions for the reproduction number  $\mathcal{R}$ , as well as the values of parameters, given in Table 1, as our baseline parameter values to obtain and present the results Figure 7. We do not include studies with the parameter  $\alpha$ , as the elasticity index,  $|\mathcal{F}_\alpha^{\mathcal{R}}| < .03$  even for  $\alpha = 1$ .

Figure 7 graphically illustrates the elasticity of the reproduction number  $\mathcal{R}$ , with respect to PrEP-specific control parameters:  $\theta$ ,  $\sigma$ ,  $q$  for 8 different scenarios of PrEP initiation rates, suspension rates, and adherence. Respectively these elasticities are given by  $\mathcal{F}_\theta^{\mathcal{R}}$ ,  $\mathcal{F}_\sigma^{\mathcal{R}}$ , and  $\mathcal{F}_q^{\mathcal{R}}$ . The rest of the parameters are assumed to have values listed in Table 1. The bar labelled a in the legend of Figure 7 corresponds to the elasticity of the baseline values for the parameters ( $\theta$ ,  $\sigma$ ,  $q$ ). The elasticity with respect to  $\theta$  and  $q$  are negative indicating that as more individuals take PrEP and are more compliant, the reproduction number decreases. Similarly as  $\sigma$  increases, fewer individuals are taking PrEP and the reproduction number increases. For example, consider  $\mathcal{F}_\theta^{\mathcal{R}}$  (bar a). For every 10% increase in  $\theta$ , the PrEP initiation rate, the reproduction number will decrease by 2% when  $\theta$ ,  $\sigma$ , and  $q$ , are at baseline values.

The first four bars, a-d, for each of the elasticities,  $\mathcal{F}_\theta^{\mathcal{R}}$ ,  $\mathcal{F}_\sigma^{\mathcal{R}}$ , and  $\mathcal{F}_q^{\mathcal{R}}$ , evaluated at the baseline adherence rate of 50%. The elasticity indices  $\mathcal{F}_\theta^{\mathcal{R}}$  are  $\mathcal{F}_\sigma^{\mathcal{R}}$  are small. At 50% adherence,  $q = .5$ , even a 40% initiation rate and minimal 10% discontinuation rate (bar d) gives only a 1% change in the reproduction number given a 10% change in both  $\theta$  and  $\sigma$ . When the adherence level is increased from 50% (as in bars labelled a-d) to 75% (as in

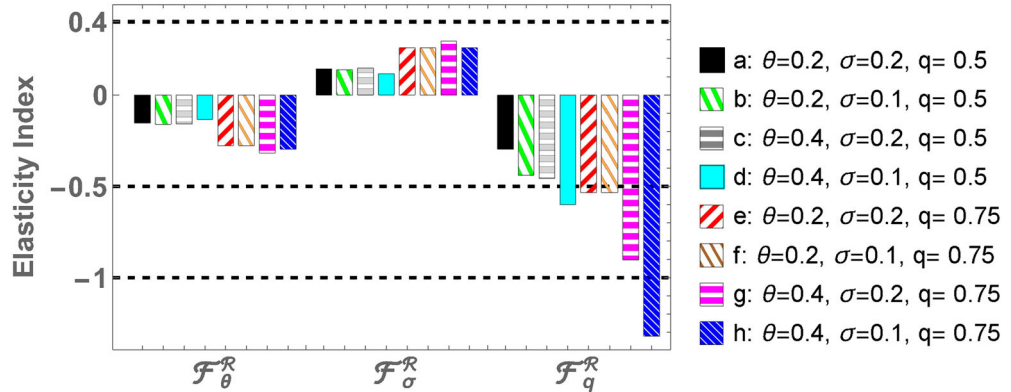


**Figure 7.** Elasticity of the reproduction number  $\mathcal{R}$ , with respect to PrEP-specific control parameters:  $\theta, \sigma, q$ . Elasticity (normalized forward sensitivity) indices were calculated for 8 different scenarios (a-h) of PrEP initiation rates, discontinuation rates and adherence levels. The rest of the parameters are assumed to have the baseline values listed in Table 1.

bars labelled e-h), the 40% initiation rate and minimal 10% discontinuation rate (bar h) increase to a 3% change in the reproduction number given a 10% change in both  $\theta$  and  $\sigma$ . This shows that the reproduction number is not very sensitive to the PrEP initiation and discontinuation rates. However, the reproduction number and the elasticity index  $\mathcal{F}_q^R$  are more sensitive to the PrEP schedule adherence,  $q$ . At the level of a 40% initiation rate and minimal 10% discontinuation rate with 50% adherence (bar d) we see that a 10% increase in adherence ( $\mathcal{F}_q^R$ ) will result in over a 5% decrease in the reproduction number. With a 40% initiation rate, 20% discontinuation rate, and 75% adherence level (bar g), a 10% change in the adherence ( $\mathcal{F}_q^R$ ) will lead to almost a 10% decrease in the reproduction number. If we can reduce the discontinuation rate to 10% (bar h), then a 10% change in the adherence ( $\mathcal{F}_q^R$ ) will lead to a 13% decrease in the reproduction number. This indicates that a campaign to improve PrEP adherence will be more effective than a campaign to increase initiation or decrease discontinuation rates.

Figure 8 illustrates the elasticity index for varying values of the PrEP parameters. The first column of contour graphs in the figure corresponds to the baseline values of the parameters  $\sigma, q, \theta$ . The first row, Figure 8(a), decreases  $\sigma$  from 0.2 to 0.05 as in Figure 5(a). The second row, Figure 8(b), increases  $q$  from 0.5 to 0.9 as illustrated in the contour plots in Figure 5(b). The third row, Figure 8(c), corresponds to increasing  $\theta$  from the baseline value of 0.05 to 0.4. Note that while the previous figure illustrates the value of the reproduction number, these plots indicate the impact of a small change in the parameter will have on the reproduction number. Note the difference in magnitude between the three rows. The rows(a) and (b) have magnitudes on the order of single digits, whereas the row (c) is an order of magnitude smaller. Thus, impacts on decreasing the reproduction number are more significant in rows (a) and (b). The largest impact comes from small  $\sigma$  and large values of  $q$  and  $\theta$ , however, the colour scales correspond to negative values which indicate that the reproduction number would decrease. For the previously identified values of the parameters  $\sigma = 0.1, q = 0.75$  and  $\theta = 0.2$  the index is approximately  $-1$ .

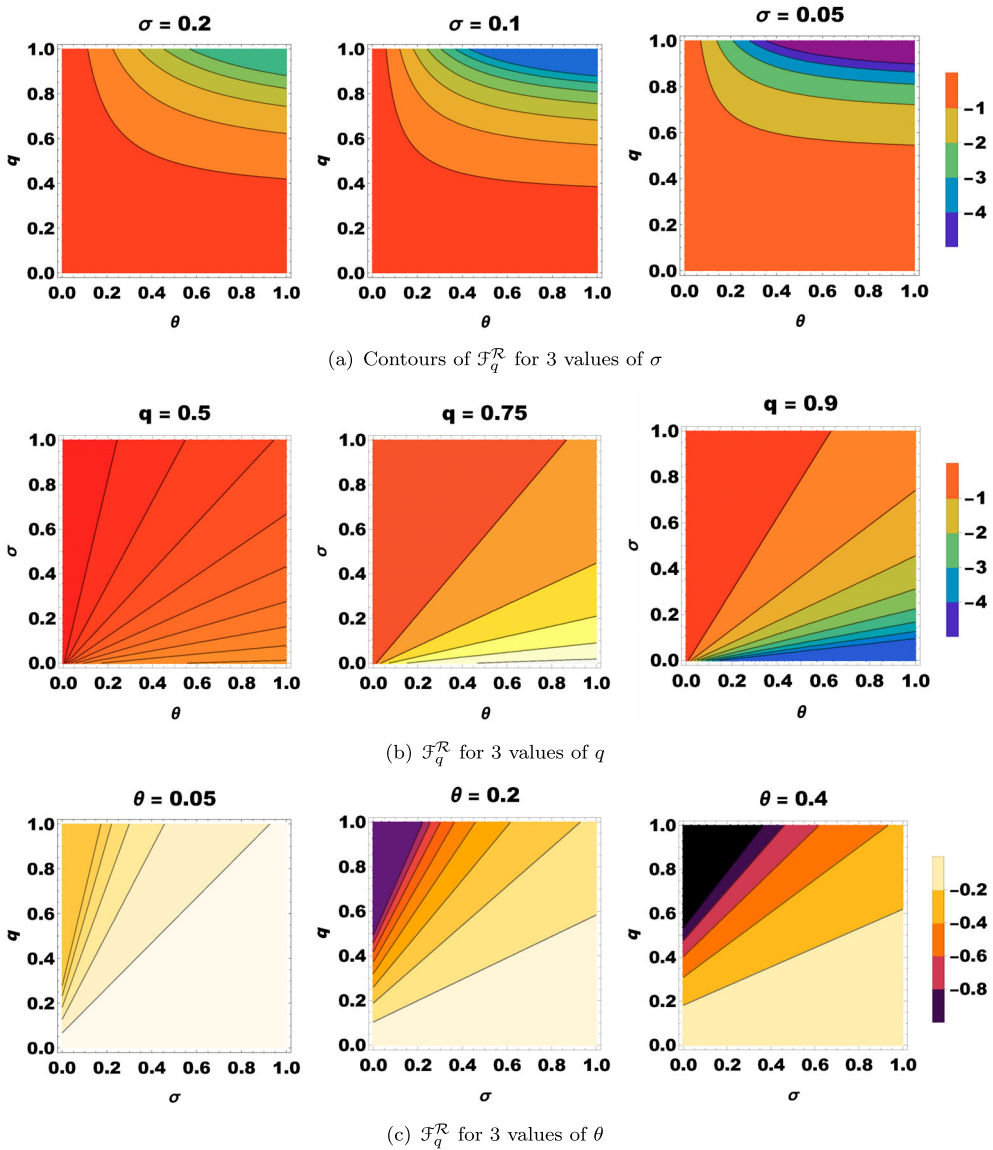


**Figure 8.**  $\mathcal{F}_q^R$ : Changes in elasticity of reproductive number  $\mathcal{R}$  with respect to PrEP treatment adherence  $q$ . The contours indicate the values of elasticity indices  $\mathcal{F}_q^R$ . Row 1 shows the dependence of  $\mathcal{F}_q^R$  for 3 values of  $\sigma$ . Row 2 shows the dependence of  $\mathcal{F}_q^R$  for 3 values of  $q$ . Row 3 shows the dependence of  $\mathcal{F}_q^R$  for 3 values of  $\theta$ . The first column has the baseline values with the second and third columns showing the potential of tighter controls.

## 8. Discussion

We developed a *PSI* model for MSM HIV transmission with a constant population including possibly non-monogamous long-term partnerships. The rate of infection is calculated using Markov chain theory and complicated by allowing individuals to transition between the susceptible population not taking PrEP and the susceptible population taking PrEP.

Including differential susceptibility with non-monogamous long-term partnerships is a novel contribution to the literature. The inclusion of possibly non-monogamous partnerships allows for the inclusion of HIV transmission through either casual sex or through concurrent long-term partnerships. We show that our model approximates the percentage of HIV negative MSM taking PrEP within a 90% confidence interval. Our mathematical method of determining that contribution by using Markov chain theory to evaluate the mean value of the long-term partnerships in a deterministic system of ordinary differential equations is also novel.

The reproduction number for this model is calculated and its dependence on the PrEP parameters of initiation, suspension and adherence is analysed. Additionally, the sensitivity index (or elastic index) of the reproduction number on the PrEP parameters is analysed for varying values of  $\theta, \sigma, q$ . LHS and PRCC values of the PrEP parameters indicate approximately the same sensitivity with respect to the reproduction number. We also included in the model a parameter  $\alpha$  which corresponds to the fraction of the incoming population that initiates PrEP treatment before becoming sexually active. This parameter did not play a significant role in the magnitude of the reproduction number or the corresponding sensitivity analysis of the reproduction number. However, the parameter  $\alpha$  does appear in the endemic equilibrium and should affect the overall fraction of infected individuals with respect to the total population.

We explored the effect of varying the  $\theta, \sigma, q$  parameters on the reproduction number. The elasticity indices indicate the sensitivity of the reproduction number to parameter changes. We can see not only the reduction in the reproduction number but also which parameter has the largest effect in reducing the number of new HIV cases. While current adherence estimates are approximately 50%, increasing adherence of the PrEP dosage regimen to the level of 75% would significantly decrease the reproduction number and decrease the (negative) elastic index with respect to adherence. For adherence of 75%, increasing the current PrEP initiation rate  $\theta$  from 5% to 40% and decreasing the PrEP suspension rate from a baseline 20% to 10% also significantly impacts the reproduction number. This indicates that a campaign to increase daily adherence will have a larger effect than just increasing the rate at which individuals initiate PrEP and decreasing the rate at which individuals discontinue PrEP. As expected, increasing adherence and initiation while decreasing discontinuation would have the greatest impact in lowering the reproduction number.

Similar conclusions about the importance of daily adherence was found in both Jenness et al. [14] and Tollett et al. [22] for non-constant populations. Both Jenness et al. and Tollett et al. separated the MSM population into high risk and low risk populations (as defined by the CDC), assumed only the high risk population is using PrEP, and that once an individual starts taking PrEP, they do not discontinue its use. Neither model contained the combination of casual partnerships and long-term non-monogamous partnerships. Jenness et al. [14] used a network-based model of HIV in a population of MSM parameterized by data from the entire United States. By tracking uniquely identifiable sexual partnership dyads in this study, Jenness et al. [14] estimated the percentage of infections averted and the number of MSM needed to treat under behavioural indications of the CDC's PrEP guidelines for high risk individuals. They found that increasing the coverage in the high risk category to 40% with a 62% adherence, averted 33% of new HIV infections. Reductions to the number of MSM needed to treat were associated with better adherence but not with

the number of individuals taking PrEP. Tollett et al. [22] used a population model based on MSM data from Arizona. Their model predicts a 22% (50%) reduction in new HIV cases, with an adherence of 50% (80%), respectively. We note that a measure of coverage is the net difference between PrEP initiation and PrEP discontinuation. We separate these two pieces and illustrate that each impacts the reproduction number differently. Since our model does not distinguish between high and low risk individuals, the net difference in our case does not completely align with coverage results of [14, 22]. While our model does not directly predict percentage of infections averted, we similarly conclude that adherence reduces both the reproduction number and the elasticity indices with respect to adherence, initiation and discontinuation. A decrease in the reproduction number is associated with a decrease in the number of new infections. By focussing our analysis on the reproduction number, we are able to identify specific levels of adherence, initiation and discontinuation in order to eliminate new HIV cases.

There are a few limitations of this model. It would be essential to add a non-constant population and disease death over a long period of time or in a country without a high level of highly active retroviral therapy. An exploration of this idea in a model with long-term partnerships and staged infection without PrEP was considered in [68]. In addition, a non-constant population allows the possibility of a backward bifurcation, that is, a stable endemic equilibrium when  $\mathcal{R} < 1$ , for an example on a PrEP model see [22]. We also did not consider PrEP on demand, which is becoming increasingly available, and hence could have an impact on HIV dynamics. The incubation period of HIV is 2-4 weeks, which we did not consider with this model. We also assumed that infectivity decreased relative to the product of adherence and effectiveness of PrEP. More general dependencies could be considered.

## Acknowledgments

The authors thank the reviewers for their comments that led to improvements in this paper.

## Disclosure statement

No potential conflict of interest was reported by the author(s).

## Funding

The authors were supported by the National Science Foundation (NSF) [grant number DMS-2000044].

## References

- [1] Centers for Disease Control and Prevention. HIV surveillance report 2019; 2021. Available from: <https://www.cdc.gov/hiv/library/reports/hiv-surveillance.html>
- [2] Centers for Disease Control and Prevention (CDC). HIV in the United States and dependent areas; 2019. Available from: <https://www.cdc.gov/hiv/statistics/overview/ataglance.html>
- [3] Centers for Disease Control and Prevention (CDC). HIV Surveillance report, 2019; 2021. Available from: <https://www.cdc.gov/hiv/pdf/library/reports/surveillance/cdc-hiv-surveillance-supplemental-report-vol-26-1.pdf>
- [4] Foley BT, Korber BTM, Leitner TK, et al. HIV sequence compendium 2018, Los Alamos: NM (USA); 2018. (Tech. Rep., Los Alamos National Lab.(LANL)).

- [5] Centers for Disease Control and Prevention. [cited 2023 Jan 22]. Available from: <https://www.cdc.gov/nchhstp/newsroom/fact-sheets/hiv/PrEP-for-hiv-prevention-in-the-US-factsheet.html>
- [6] Franks J, Hirsch-Movarman Y, Loquere AS, et al. Sex, PrEP, and stigma: experiences with HIV pre-exposure prophylaxis among New York city MSM participating in the HPTN 067/ADAPT study. *AIDS and Behavior*. 2018;22:1139–1149. doi: [10.1007/s10461-017-1964-6](https://doi.org/10.1007/s10461-017-1964-6)
- [7] S McCormack, DT Dunn, M Desai, et al. Pre-exposure prophylaxis to prevent the acquisition of HIV-1 infection (PROUD): effectiveness results from the pilot phase of a pragmatic open-label randomised trial. *The Lancet*. 2016;387:53–60. doi: [10.1016/S0140-6736\(15\)00056-2](https://doi.org/10.1016/S0140-6736(15)00056-2)
- [8] JM Molina, C Capitant, B Spire, et al. On-demand preexposure prophylaxis in men at high risk for HIV-1 infection. *N Engl J Med*. 2015;373:2237–2246. doi: [10.1056/NEJMoa1506273](https://doi.org/10.1056/NEJMoa1506273)
- [9] R Tetteh, B Yankey, E Nartey, et al. Pre-exposure prophylaxis for HIV prevention: safety concerns. *Drug Saf*. 2017;40:273–283. doi: [10.1007/s40264-017-0505-6](https://doi.org/10.1007/s40264-017-0505-6)
- [10] World Health Organization. Adherence to long-term therapies: evidence for action; 2003. Available from: <https://iris.who.int/handle/10665/42682>
- [11] Centers for Disease Control and Prevention (CDC). Preexposure prophylaxis for the prevention of HIV infection in the United States – 2017 update: a clinical practice guideline; 2018. Available from: <https://www.cdc.gov/hiv/pdf/risk/prep/cdc-hiv-prep-guidelines-2017.pdf>
- [12] World Health Organization. Differentiated and simplified pre-exposure prophylaxis for HIV prevention: update to WHO implementation guidance (Tech. Rep.). World Health Organization; 2022.
- [13] DK Smith, M Van Handel, RJ Wolitski, et al. Vital signs: estimated percentages and numbers of adults with indications for preexposure prophylaxis to prevent HIV acquisition – United States, 2015. *Morb Mortal Wkly Rep*. 2015;64:1291–1295. doi: [10.15585/mmwr.mm6446a4](https://doi.org/10.15585/mmwr.mm6446a4)
- [14] SM Jenness, SM Goodreau, E Rosenberg, et al. Impact of the centers for disease control's HIV preexposure prophylaxis guidelines for men who have sex with men in the United States. *J Infect Dis*. 2016;214:1800–1807. doi: [10.1093/infdis/jiw223](https://doi.org/10.1093/infdis/jiw223)
- [15] Centers for Disease Control and Prevention. Monitoring selected national HIV prevention and care objectives by using HIV surveillance data—United States and 6 territories and freely associated states, 2022. hiv surveillance supplemental report; 2024. Available from: <https://www.cdc.gov/hiv-data/nhss/national-hiv-prevention-and-care-outcomes.html>
- [16] S Kim, M Yoon, N Ku, et al. Mathematical modeling of HIV prevention measures including pre-exposure prophylaxis on HIV incidence in South Korea. *PLoS ONE*. 2014;9:e90080. doi: [10.1371/journal.pone.0090080](https://doi.org/10.1371/journal.pone.0090080)
- [17] N Punyacharoensin, WJ Edmunds, D De Angelis, et al. Modelling the HIV epidemic among MSM in the United Kingdom: quantifying the contributions to HIV transmission to better inform prevention initiatives. *AIDS*. 2015;29:339–349. doi: [10.1097/QAD.0000000000000525](https://doi.org/10.1097/QAD.0000000000000525)
- [18] N Punyacharoensin, WJ Edmunds, D De Angelis, et al. Effect of pre-exposure prophylaxis and combination HIV prevention for men who have sex with men in the UK: a mathematical modelling study. *The Lancet HIV*. 2016;3:e94–e104. doi: [10.1016/S2352-3018\(15\)00056-9](https://doi.org/10.1016/S2352-3018(15)00056-9)
- [19] J Li, L Peng, S Gilmour, et al. A mathematical model of biomedical interventions for HIV prevention among men who have sex with men in China. *BMC Infect Dis*. 2018;18:1–9. doi: [10.1186/s12879-017-2892-9](https://doi.org/10.1186/s12879-017-2892-9)
- [20] CJ Silva, DF Torres. Modeling and optimal control of HIV/AIDS prevention through PrEP. *Discrete Continuous Dyn Syst – S*. 2017;11:119–141. doi: [10.3934/dcdss.2018008](https://doi.org/10.3934/dcdss.2018008)
- [21] Z Chazuka, E Mudimu, D Mathebula. Stability and bifurcation analysis of an HIV model with pre-exposure prophylaxis and treatment interventions. *Sci Afr*. 2024;23:e01979.
- [22] Q Tollett, S Safdar, A Gumel. Dynamics of a two-group model for assessing the impacts of pre-exposure prophylaxis, testing and risk behaviour change on the spread and control of HIV/AIDS in an MSM population. *Infect Dis Model*. 2023;9:103–127.
- [23] B Steinegger, I Iacopini, AS Teixeira, et al. Non-selective distribution of infectious disease prevention may outperform risk-based targeting. *Nat Commun*. 2022;13:3028. doi: [10.1038/s41467-022-30639-3](https://doi.org/10.1038/s41467-022-30639-3)

- [24] D Hansson, S Strömdahl, KY Leung, et al. Introducing pre-exposure prophylaxis to prevent HIV acquisition among men who have sex with men in Sweden: insights from a mathematical pair formation model. *BMJ Open*. **2020**;10:e033852. doi: [10.1136/bmjopen-2019-033852](https://doi.org/10.1136/bmjopen-2019-033852)
- [25] Q Tollett. Mathematics of transmission dynamics and control of HIV/AIDS in an MSM population [Ph.D. diss.]. Arizona State University, Tempe, AZ; 2023.
- [26] TH Whitfield, SA John, HJ Rendina, et al. Why I quit pre-exposure prophylaxis (PrEP)? A mixed-method study exploring reasons for PrEP discontinuation and potential re-initiation among gay and bisexual men. *AIDS Behav*. **2018**;22:3566–3575. doi: [10.1007/s10461-018-2045-1](https://doi.org/10.1007/s10461-018-2045-1)
- [27] K Weiss, P Prasad, T Sanchez, et al. Association between HIV PrEP indications and use in a national sexual network study of US men who have sex with men. *J Int AIDS Soc*. **2021**;24e25826. doi: [10.1002/jia2.v24.10](https://doi.org/10.1002/jia2.v24.10)
- [28] E Rosenberg, P Sullivan, E DiNenno, et al. Number of casual male sexual partners and associated factors among men who have sex with men: results from the national HIV behavioral surveillance system. *BMC Public Health*. **2011**;11:189–198. doi: [10.1186/1471-2458-11-189](https://doi.org/10.1186/1471-2458-11-189)
- [29] J Chapin-Bardales, ES Rosenberg, PS Sullivan, et al. Trends in number and composition of sex partners among men who have sex with men in the United States, national HIV behavioral surveillance, 2008–2014. *J Acquir Immune Defic Syndr*. **2019**;81:257.265 doi: [10.1097/QAI.0000000000002025](https://doi.org/10.1097/QAI.0000000000002025)
- [30] M Kretzschmar, J Heijne. Pair formation models for sexually transmitted infections: a primer. *Infect Dis Model*. **2017**;2:368–378.
- [31] C Kuehn. Moment closure—a brief review. In: Schöll E, Klapp S, and P Hövel, editors. *Control of self-organizing nonlinear systems. Understanding complex systems*. Cham: Springer; 2016. p. 253–271.
- [32] K Gurski. A sexually transmitted infection model with long-term partnerships in homogeneous and heterogenous populations. *Infect Dis Model*. **2019**;4:142–160.
- [33] K Gurski, K Hoffman, S Gutowska, et al. Modeling HIV and HSV-2 using partnership models. In: Cantrell S, Martcheva M, Neval A, Ruan S, and Shuai Z, editors. *Contemporary research in mathematical biology*. World Scientific; 2025. doi: [10.1142/12639](https://doi.org/10.1142/12639)
- [34] GB Gomez, A Borquez, CF Caceres, et al. The potential impact of pre-exposure prophylaxis for HIV prevention among men who have sex with men and transwomen in Lima, Peru: a mathematical modelling study. *PLoS Med*. **2012**;9:e1001323. doi: [10.1371/journal.pmed.1001323](https://doi.org/10.1371/journal.pmed.1001323)
- [35] S Lee, J Ko, X Tan, et al. Markov chain modelling analysis of HIV/AIDS progression: a race-based forecast in the United States. *Indian J Pharm Sci*. **2014**;76:107.
- [36] WY Tan, Z Xiang. A state space model for the HIV epidemic in homosexual populations and some applications. *Math Biosci*. **1998**;152:29–61. doi: [10.1016/S0025-5564\(98\)10013-5](https://doi.org/10.1016/S0025-5564(98)10013-5)
- [37] C Twumasi, L Asiedu, EN Nortey. Markov chain modeling of HIV, tuberculosis, and hepatitis B transmission in Ghana. *Interdisciplinary Perspect Infect Dis*. **2019**;2019:9362492.
- [38] N Yamamoto, Y Koizumi, S Tsuzuki, et al. Evaluating the cost-effectiveness of a pre-exposure prophylaxis program for HIV prevention for men who have sex with men in Japan. *Sci Rep*. **2022**;12:3088. doi: [10.1038/s41598-022-07116-4](https://doi.org/10.1038/s41598-022-07116-4)
- [39] S Gutowska, K Hoffman, K Gurski. The effect of PrEP uptake and adherence on the spread of HIV in the presence of casual and long-term partnerships. *Math Biosci Eng*. **2022**;19:11903–11934. doi: [10.3934/mbe.2022255](https://doi.org/10.3934/mbe.2022255)
- [40] L Simpson, AB Gumel. Mathematical assessment of the role of pre-exposure prophylaxis on HIV transmission dynamics. *Appl Math Comput*. **2017**;293:168–193.
- [41] T Straubinger, K Kay, R Bies. Modeling HIV pre-exposure prophylaxis. *Front Pharmacol*. **2020**;10:1514. doi: [10.3389/fphar.2019.01514](https://doi.org/10.3389/fphar.2019.01514)
- [42] RM Anderson, RM May. *Infectious diseases of humans: dynamics and control*. Oxford (UK): Oxford Science Publications; 1991.
- [43] NIDA, What is HAART?; 2020. Available from: <https://nida.nih.gov/publications/research-reports/hivaids/what-haart>

- [44] LT Dean, HY Chang, WC Goedel, et al. Novel population-level proxy measures for suboptimal HIV preexposure prophylaxis initiation and persistence in the USA. *AIDS*. **2021**;35:2375–2381. doi: [10.1097/QAD.0000000000003030](https://doi.org/10.1097/QAD.0000000000003030)
- [45] KC Coy, RJ Hazen, HS Kirkham, et al. Persistence on HIV preexposure prophylaxis medication over a 2-year period among a national sample of 7148 PrEP users, United States, 2015 to 2017. *J Int AIDS Soc*. **2019**;22:e25252. doi: [10.1002/jia2.2019.22.issue-2](https://doi.org/10.1002/jia2.2019.22.issue-2)
- [46] AS Fauci, RR Redfield, G Sigounas, et al. Ending the HIV epidemic: a plan for the United States. *JAMA*. **2019**;321:844–845. doi: [10.1001/jama.2019.1343](https://doi.org/10.1001/jama.2019.1343)
- [47] E Jacobson, K Hicks, J Carrico, et al. Optimizing HIV prevention efforts to achieve EHE incidence targets. *J Acquir Immune Defic Syndr*. **2022**;89:374–380. doi: [10.1097/QAI.00000000000002885](https://doi.org/10.1097/QAI.00000000000002885)
- [48] K Weiss, S Goodreau, M Morris, et al. Egocentric sexual networks of men who have sex with men in the United States: results from the ARTnet study. *Epidemics*. **2020**;30:100386. doi: [10.1016/j.epidem.2020.100386](https://doi.org/10.1016/j.epidem.2020.100386)
- [49] DK Smith, JH Herbst, X Zhang, et al. Condom effectiveness for HIV prevention by consistency of use among men who have sex with men in the United States. *JAIDS J Acquir Immune Defic Syndr*. **2015**;68:337–344. doi: [10.1097/QAI.0000000000000461](https://doi.org/10.1097/QAI.0000000000000461)
- [50] K Gurski, K Hoffman. Influence of concurrency, partner choice, and viral suppression on racial disparity in the prevalence of HIV infected women. *Math Biosci*. **2016**;282:91–108. doi: [10.1016/j.mbs.2016.09.009](https://doi.org/10.1016/j.mbs.2016.09.009)
- [51] M von Cube, M Schumacher, M Wolkewitz. Basic parametric analysis for a multi-state model in hospital epidemiology. *BMC Med Res Methodol*. **2017**;17:1–12. doi: [10.1186/s12874-017-0379-4](https://doi.org/10.1186/s12874-017-0379-4)
- [52] H Pishro-Nik. Introduction to probability, statistics and random processes. Kappa Research, LLC; **2014**. <https://www.probabilitycourse.com/>
- [53] D Cox, H Miller. The theory of stochastic processes. Vol. 134. New York: Routledge; **1977**.
- [54] R Brinks, A Hoyer. Illness-death model: statistical perspective and differential equations. *Lifetime Data Anal*. **2018**;24:743–754. doi: [10.1007/s10985-018-9419-6](https://doi.org/10.1007/s10985-018-9419-6)
- [55] G Rodriguez. Multivariate survival models. Princeton University; **2005**. (Lectures Notes).
- [56] C Castillo-Chavez, Z Feng, W Huang. On the computation of  $R_0$  and its role on global stability. *Math Approac Emerg Reemerg Infect Diseas: An Introd*. **2002**;1:229. doi: [10.1007/978-1-4757-3667-0](https://doi.org/10.1007/978-1-4757-3667-0)
- [57] CA Koss, ED Charlebois, J Ayieko, et al. Uptake, engagement, and adherence to pre-exposure prophylaxis offered after population HIV testing in rural Kenya and Uganda: 72-week interim analysis of observational data from the SEARCH study. *The Lancet HIV*. **2020**;7:e249–e261. doi: [10.1016/S2352-3018\(19\)30433-3](https://doi.org/10.1016/S2352-3018(19)30433-3)
- [58] JT Parsons, HJ Rendina, JM Lassiter, et al. Uptake of HIV pre-exposure prophylaxis (PrEP) in a national cohort of gay and bisexual men in the United States: the motivational PrEP cascade. *J AIDS* (1999). **2017**;74:285.
- [59] R Chou, C Evans, A Hoverman, et al. Preexposure prophylaxis for the prevention of HIV infection: evidence report and systematic review for the US preventive services task force. *JAMA*. **2019**;321:2214–2230. doi: [10.1001/jama.2019.2591](https://doi.org/10.1001/jama.2019.2591)
- [60] Centers for Disease Control and Prevention. Monitoring selected national HIV prevention and care objectives by using HIV surveillance data—United States and 6 dependent areas—2015. *HIV Surveillance Supplemental Report*, 2017 (Tech. Rep.). U.S. Department of Health and Human Services, Centers for Disease Control and Prevention; 2017.
- [61] R Stephenson, A Bratcher, M Mimiaga, et al. Brief report: accuracy in self-report of viral suppression among HIV-positive men with HIV-negative male partners. *J Acquir Immune Defic Syndr*. **2020**;83:210–214. doi: [10.1097/QAI.0000000000002240](https://doi.org/10.1097/QAI.0000000000002240)
- [62] Centers for Disease Control and Prevention. *HIV/AIDS Surveillance Report*, 2005 (Tech. Rep. Rev. Ed.). U.S. Department of Health and Human Services, Centers for Disease Control and Prevention; 2007.
- [63] Centers for Disease Control and Prevention; 2022. [cite 2022 Dec 1]. Available from: <https://www.cdc.gov/hiv/library/reports/hiv-surveillance.html>

- [64] AIDSVu.org. Mapping PrEP: First ever data on PrEP users across the U.S.; 2018 [cited 2024 Jun 6]. Available from: <https://aidsvu.org/prep/>
- [65] Centers for Disease Control and Prevention. Core indicators for monitoring the ending the HIV epidemic initiative (preliminary data): national HIV surveillance system data reported through june 2021; and preexposure prophylaxis (PrEP) data reported through march 2021. HIV surveillance data tables; 2021. Available from: <https://www.cdc.gov/hiv/library/reports/hiv-surveillance.html>
- [66] I Holloway, E Krueger, I Meyer, et al. Longitudinal trends in PrEP familiarity, attitudes, use and discontinuation among a national probability sample of gay and bisexual men, 2016–2018. *PLoS One*. **2020**;15:e0244448. doi: [10.1371/journal.pone.0244448](https://doi.org/10.1371/journal.pone.0244448)
- [67] RL Iman, JC Helton. An investigation of uncertainty and sensitivity analysis techniques for computer models. *Risk Anal*. **1988**;8:71–90. doi: [10.1111/risk.1988.8.issue-1](https://doi.org/10.1111/risk.1988.8.issue-1)
- [68] K Gurski, K Hoffman. Staged HIV transmission and treatment in a dynamic model with long-term partnerships. *J Math Biol*. **2023**;86:74. doi: [10.1007/s00285-023-01885-w](https://doi.org/10.1007/s00285-023-01885-w)